Revista Brasileira de Geofísica
RBGf
Brazilian Journal of Geophysics

Revista Brasileira de Geofísica (2007) 25(4): 363-387

ISSN 0102-261X
www.scielo.br/rbg

OCEANOGRAPHIC CHARACTERISTICS OF BAÍA DE TODOS OS SANTOS, BRAZIL

Mauro Cirano[1] and Guilherme Camargo Lessa[2]

Recebido em 18 novembro, 2006 / Aceito em 9 outubro, 2007
Received on November 18, 2006 / Accepted on October 9, 2007

ABSTRACT. Based on a vast set of *in situ* data, a first comprehensive overview of the oceanographic characteristics of Baía de Todos os Santos (BTS) is provided. BTS is the second largest coastal bay in Brazil (maximum area of 1223 km^2 and average depth of 9.8 m), and is located in the northeast Brazil, in the vicinity of Salvador city. The circulation inside the bay is mostly tidally driven and does not vary significantly throughout the year. On the other hand, the wet (winter) and dry (summer) seasons does alter significantly the distribution of water properties inside the BTS. During summer, the waters inside the bay have oceanic characteristics, with Tropical Water (TW) penetrating along the whole region, except for the mouth of Rio Paraguaçu. The water temperature inside the bay is higher than in the coastal zone, and variations can be up to 3°C, reaching a maximum of nearly 30°C. During winter, with the increase of freshwater inflow, salinity variations of about 4 are observed between the innermost stations inside BTS and the adjacent coastal region. Salinity values inside the bay can be as low as 32.3, inhibiting the penetration of TW into the BTS, which is totally occupied by a locally formed Coastal Water (CW). An evaluation of the flushing time is also provided and shows that during summer, a 60-fold increase can be observed compared to winter (38 days). While the circulation does not vary seasonally inside the bay, the associated inner shelf is characterized by two different scenarios. During summer, the upwelling favorable easterlies drive a southwestward flow, while during winter the more frequent occurrence of cold fronts (southerly winds) tend to reverse the circulation.

Keywords: Baía de Todos os Santos, circulation, tides, water masses.

RESUMO. Com base em um amplo conjunto de dados *in situ*, este artigo apresenta uma primeira caracterização oceanográfica da Baía de Todos os Santos. A BTS é a segunda maior baía costeira do Brasil (área máxima de 1223 km^2 e profundidade média de 9,8 m), e está localizada na região nordeste do Brasil, nas proximidades da cidade de Salvador. A circulação no interior da baía é predominantemente forçada pelas marés e não varia significantemente ao longo do ano. Por outro lado, as estações chuvosa (inverno) e seca (verão) geram uma alteração significativa nas propriedades das águas no interior da BTS. Durante o verão, as águas dentro da baía têm características oceânicas, com a Água Tropical (AT) penetrando ao longo de toda a região, com exceção da desembocadura do Rio Paraguaçu. A temperatura da água dentro da baía é maior do que a da região costeira adjacente, e estas variações podem ser de até 3°C, atingindo um máximo de 30°C. Durante o inverno, com o aumento do aporte de água doce, variações de salinidade de cerca de 4 podem ser observadas entre a parte mais interna da BTS e a região costeira adjacente. Valores de salinidade dentro da baía podem chegar até 32,3, inibindo a penetração da AT dentro da BTS, que fica totalmente ocupada por uma água costeira formada localmente. Uma avaliação do tempo de descarga também é feita e mostra que durante o verão, o tempo de descarga pode sofrer um aumento de 60% daquele observado durante o inverno (38 dias). Apesar da circulação não variar sazonalmente no interior da baía, observa-se que a plataforma interna associada é caracterizada por dois cenários. Durante o verão, os ventos de leste, que proporcionam ressurgência, atuam para gerar correntes para sudoeste, enquanto que durante o inverno, a maior ocorrência de frentes frias (ventos de sul), tende a reverter o padrão de circulação.

Palavras-chave: Baía de Todos os Santos, circulação, marés, massas de água.

[1]Centro de Pesquisas em Geofísica e Geologia (CPGG), Universidade Federal da Bahia (UFBA), Instituto de Física, Departamento de Física da Terra e do Meio Ambiente, Campus Ondina, 40170-280 Salvador, BA, Brazil. Phone: (71) 3283-8612; Fax: (71) 3283-8501 – E-mail: mcirano@ufba.br

[2]Centro de Pesquisas em Geofísica e Geologia (CPGG), Universidade Federal da Bahia (UFBA), Instituto de Geociências, Departamento de Sedimentologia, Campus Ondina, 40170-280 Salvador, BA, Brazil. Phone: (71) 3283-8611; Fax: (71) 3283-8501 – E-mail: glessa@cpgg.ufba.br

INTRODUCTION

Like most of the southern hemisphere coastlines, the Brazilian coastline has undergone a 3 m emergence in the last 6000 years (Angulo et al., 2006), and as a result the large majority of its coastal-plain estuaries that have been filled up became river deltas. Large estuaries that still survive are generally tectonic coastal bays that have apparently undergone varying degrees of subsidence and today fringe some of the most important cities and harbor the most important ports in the country. The largest bays in Brazil are: Baía de São Marcos (BSM – 2025 km^2) in the state of Maranhão, Baía de Todos os Santos (BTS – 1233 km^2) in the State of Bahia and Baía de Paranaguá (BP – 612 km^2) in the state of Paraná. The well known Baía de Guanabara (BG) in the state of Rio de Janeiro is relatively small, with an area of 384 km^2.

BTS is located in the vicinity of the third major metropolitan area in Brazil, the city of Salvador (population of 2.7 million according to IBGE, 2006), and the largest petrochemical complex of the southern hemisphere (Camaçari Petrochemical Center). Due to its economic importance, the bay houses two commodities ports (Aratu and Salvador), with a total annual flow of 31.4×10^6 tons (ANTAQ, 2005), which represent nearly 5% of the total annual flow in Brazilian ports. In addition, there are also three outfalls in the continental shelf located northeast of the bay (two for chemical substances and one for sewage). The sewage outfall is the closest to the bay entrance and was built to have a maximum discharge of 8.3 $m^3\ s^{-1}$ (CRA, 2001). Several offshore oil and gas fields are also prospected within 100 km from the bay entrance and are presented in ANP (2007).

Except for BG (Kjerfve et al., 1997), a comprehensive overview of the oceanographic characteristics of large Brazilian bays and their surrounding coastal zone is not yet found in the scientific literature. For instance, the relevant publications for BTS are restricted to studies regarding data analysis (Wolgemuth et al., 1981; Lessa et al., 2001) and modeling of water circulation (Montenegro et al., 1999). The bay and the neighboring open coastal areas in front of Salvador have been the focus of continuous environmental monitoring programs. However, the results are unfortunately kept as technical reports with restricted circulation.

The most important and complete monitoring program for the BTS was the **Projeto Bahia Azul**. It was a massive project funded by the State Government from 1998 to 2001 to assess the water quality of the BTS. The project made use of 33 moored instruments to sample the water velocity, temperature, salinity and the pressure field for more than 15 continuous days and over two seasons[1] (summer and winter). Synoptic hydrographic cruises were also performed inside BTS to evaluate the distribution of properties in the water column and during spring and neap tidal cycles.

The main goal of this article is to produce an oceanographic characterization of the area over its seasonal variation, providing an important source of background information on the water dynamics for the various marine scientists who work in the BTS. It also intends to pose some scientific questions related to dynamical aspects of the circulation, which will be better answered by the results of numerical modeling experiments to be presented by the authors in a future work.

STUDY AREA

The BTS is centered on latitude 12°50'S and longitude 38°38'W, with an approximate maximum width (west-east axis) and length (north-south axis) of 32 km and 50 km, respectively. The geologic framework of the BTS has been determined, to a high extend, by tectonism (Cupertino & Bueno, 2005). The bay is bounded in the east and the west by Cretaceous fault lines (Falha de Maragogipe and Falha de Salvador) associated with an aborted rift valley that gave rise to the Recôncavo Basin (Fig. 1). Although the major fault systems were established in the Cretaceous, reactivation events occurred in the Tertiary and Quaternary, as indicated by King (1956), Tricart & da Silva (1968), Martin et al. (1986) and Bittencourt et al. (1999). The geomorphology of the bay is primarily dictated by tectonic alignments, but deep drainage channels ramify inside the bay following an old drainage network going towards Rio Paraguaçu, Rio Subaé and Baía de Aratu (Fig. 2). The deepest areas inside the bay, reaching depths of 70 m, are associated with the paleo-valley of Rio Paraguaçu, which is segmented (see the 20 m isobath in Figure 2) due to sediment accumulation in front of Canal do Paraguaçu and Canal de Itaparica. Significant accumulation of sediment is also observed in the ebb-tidal deltas fronting both entrances of the bay (Canal de Salvador and Canal de Itaparica).

Eleven textural facies were mapped by Dias (2004) (Fig. 3). Siliciclastic sand occurs at the bay entrance channels, along the western bay margin and close to the river mouths. The bay-mouth sand is of marine origin, while that inside Itaparica channel and along the western bay margin is originated from the erosion of sandstone deposits. Carbonate sand encircles the two central islands of Maré and Frades. Mud occurs predominantly in the

[1] The tropical humid climate, as it will be discussed later in more details, is divided in a dry and a wet season. For BTS, the summer months are part of the dry season, while the winter months are part of the wet season.

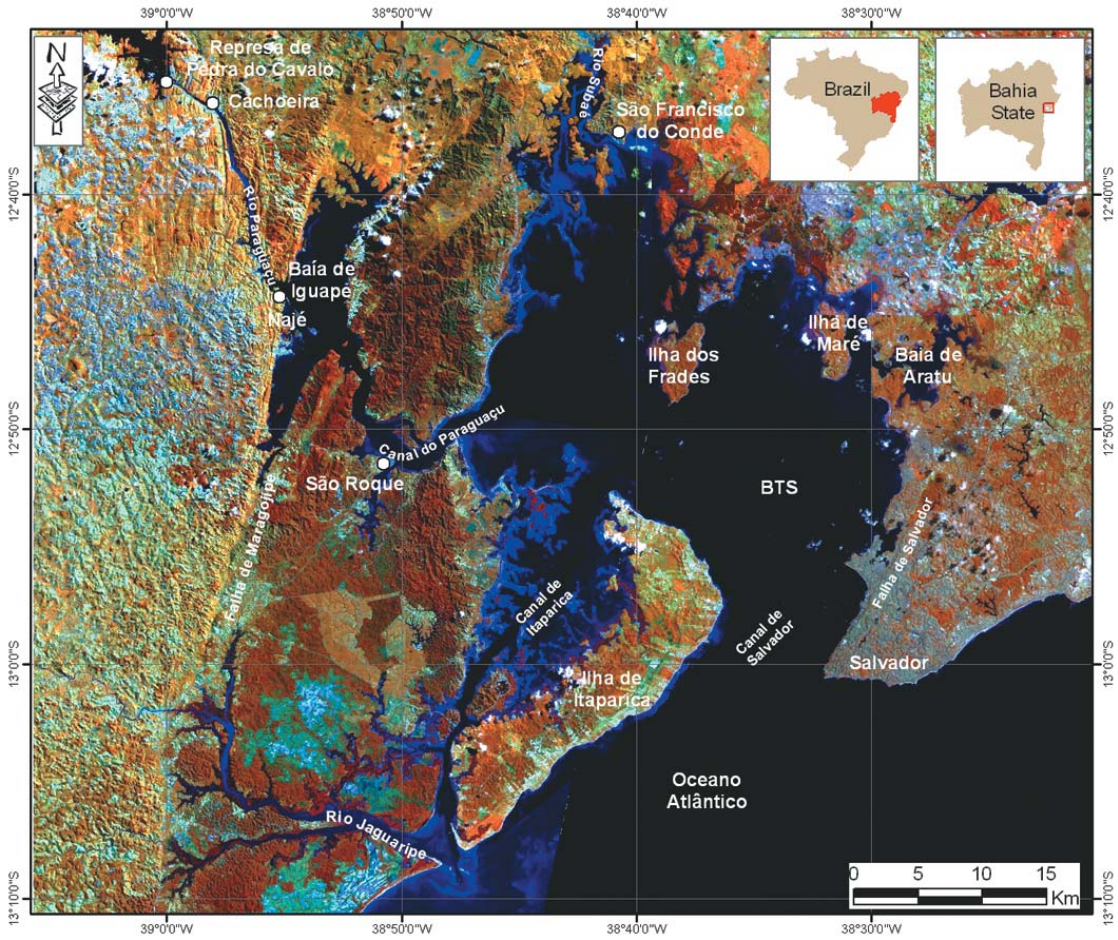

Figure 1 – Satellite image of Baía de Todos os Santos (BTS) along with the location of important landmarks and drainage channels. Fault lines that control the bay's geomorphology are oriented SW-NE.

northern half of the bay affected by the drainage of fine grained sedimentary rocks. Gravel is often observed in the fluvial delta of Rio Paraguaçu and along Canal do Paraguaçu, where it is likely associated with the exposure of lowstand fluvial deposits. Lessa et al. (2000) interpreted the sand deposits at the bay entrance as a transgressive, siliciclastic marine sand facies, and those around the island as a transgressive carbonate marine sand facies. The muddy sediments in the northern half of the bay would be related to a transgressive bay sand-mud facies and to a regressive bay-mud facies.

The maximum bay area (at an equinoctial spring tide) and its wet perimeter (based on a planimetry estimative using Landsat images with a spatial resolution of 15 m) correspond to 1223 km^2 and 1175 km, respectively. These numbers can be increased by 86 km^2 and 291 km, respectively, if the 91 islands internal to the BTS are taken into account. Overall the bay is shallow with an area-weighted depth of 9.8 m. Approximately 94% of the bay area lay above depths of 25 m. The intertidal area is 327 km^2 (or 27% of the maximum bay area), where 152 km^2 are occupied by mangroves, 160 km^2 by non-vegetated flats (with varied sediment textures) and 15 km^2 by non-vegetated supratidal flats. The bay volume during maximum spring tides is approximately 12×10^9 m^3, whereas the volume below the hydrographic datum (0 m DHN[2] or MLLW) is 8.9×10^9 m^3. This gives a maximum spring-tidal prism of about 3.1×10^9 m^3.

Climate and the hydrological cycle

The climate at the entrance of the bay is tropical humid, with an annual mean temperature, precipitation and evaporation of 25.3°C, 2086 mm and 1002 mm, respectively (Fig. 4) (INMET,

[2]Diretoria de Hidrografia e Navegação (DHN) is the Brazilian Hydrographic Authority.

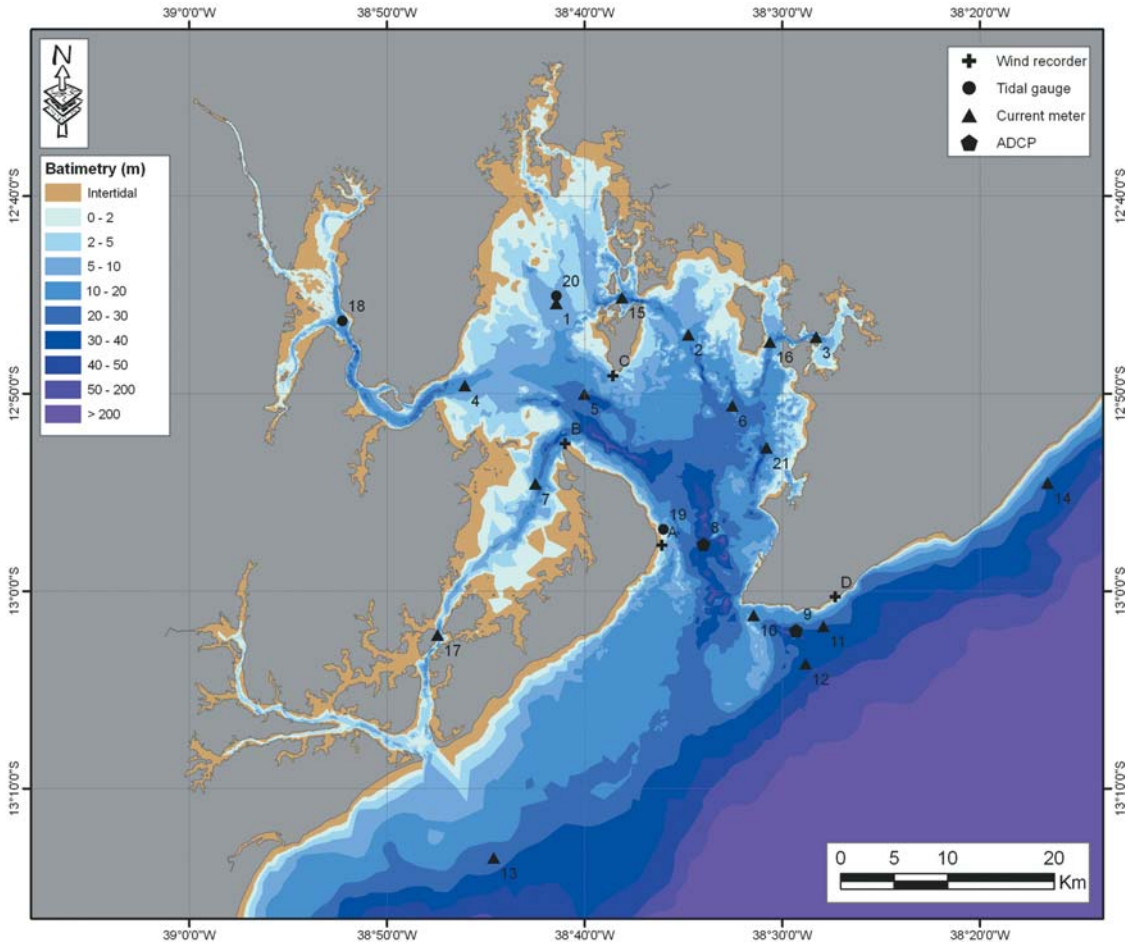

Figure 2 – Bottom topography of BTS and the location of the current meter moorings (stations 1 to 7 and 10 to 17), the ADCPs (stations 8 and 9), the meteorological stations and the tidal gauges (stations 18, 19 and 20 (at the same location of station 1)) for the winter season. The measurements during summertime were performed at the same locations, except for the station 21, which was not included. The brown areas represent the intertidal regions. The depth intervals are differentiated with colors according to the legend.

1992). A precipitation gradient of about 15 mm km^{-1} occurs westward across the bay, between Salvador and the upper reaches of Rio Paraguaçu, where the mean annual precipitation is 1200 mm. One hundred kilometers inland from the bay mouth, the climate is semi-arid, with average annual evaporation and precipitation rates of 1243 mm and 909 mm, respectively (CEPLAB, 1979).

Considering an area-weighted precipitation rate, the year-averaged volume of rain falling directly into the bay is 2.42×10^9 m^3. If the evaporation gradient across the bay is taken into account, an average volume of 0.92×10^9 m^3 is lost annually to the atmosphere (considering the area within the 0 m DHN contour). This volume must be added to the potential evapotranspiration rate from the mangroves, estimated according to the Thornthwaite method (Thornthwaite, 1948) as 1412 mm $year^{-1}$. Assuming that the real evapotranspiration in a mangrove forest equals the potential, a volume of 0.21×10^9 m^3 is also lost to the atmosphere. Hence, the atmospheric-water that enters the bay is about 1.29×10^9 m^3, which represents a year-average discharge of approximately 41 m^3 s^{-1}.

The monthly distribution of rainfall over the bay is out of phase with that in the interior. In the former, precipitation is mainly concentrated during the fall and in the beginning of the winter (March-July), when 60% of the total precipitation occurs (Fig. 4). On the other hand, the wet season in the mainland takes place between November and February. This pattern of distribution causes different inputs of freshwater inflow into the bay due to the location of the three large catchment areas, as well as the 91 small

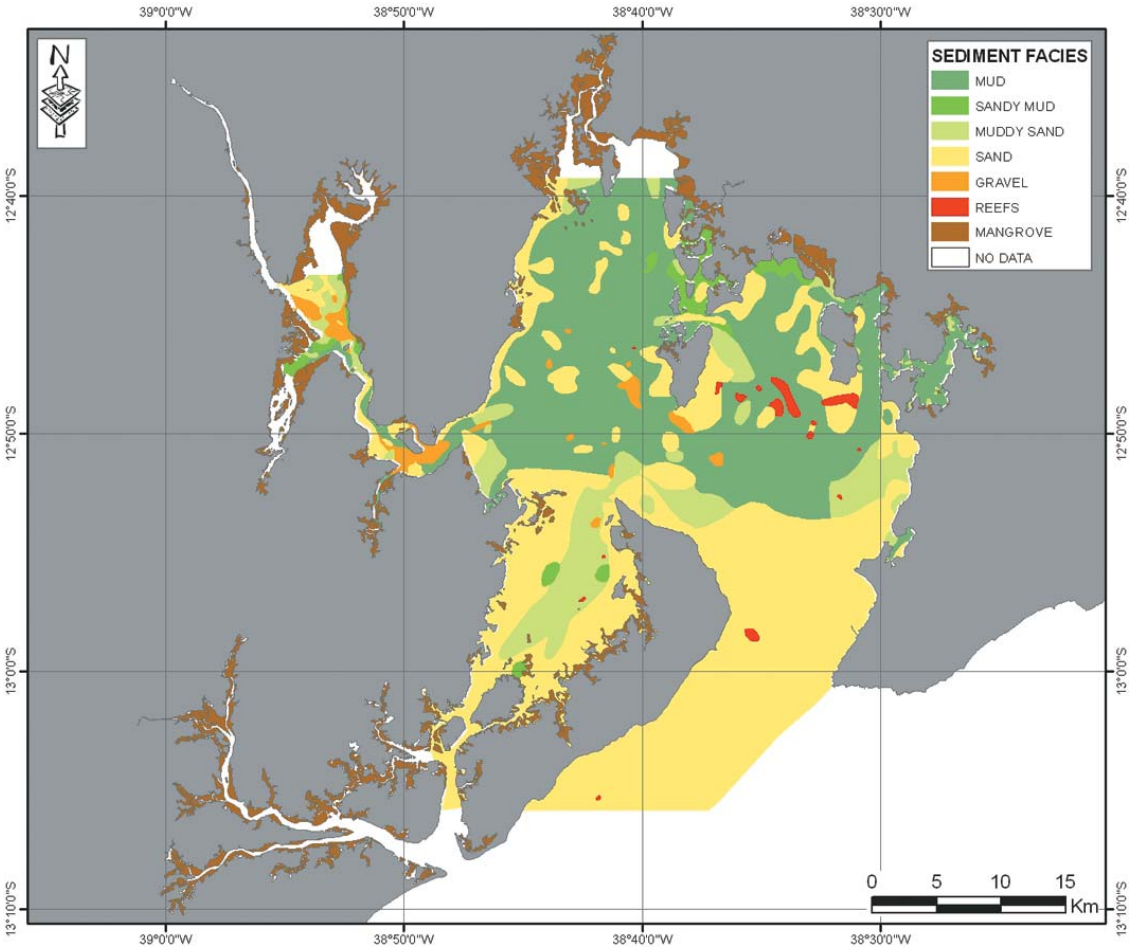

Figure 3 – Distribution of surface sediment facies inside the BTS (after Dias, 2004).

peripheral catchments (Lima & Lessa, 2002). The catchment of Rio Paraguaçu, with an area of 56,300 km^2, drains mainland rivers and provides the main point-source discharge with maxima in December and January. Between 1949 and 1986, when Pedra do Cavalo Dam (located 15 km upstream from Baía de Iguape – Figure 1) was not yet built, the mean river discharge was 90.5 m^3 s^{-1} (Genz, 2006), or 73% of the total fluvial input. After 1986, flow regulation implemented by the dam significantly altered the discharge pattern into the bay (Lima & Lessa, 2002; Genz, 2006). Based on the reservoir operational guidelines, an average daily discharge of 10 m^3 s^{-1} (in reality 60 m^3 s^{-1} in 4 hours) is released during the dry season (March-October). In the wet season (November-February), depending on the water level inside the reservoir (SRH, 1996), the discharge can reach a maximum of 1700 m^3 s^{-1}. Between 1987 and 2003, the average year river discharge dropped to 64.3 m^3 s^{-1} (Genz, 2006). Maximum mean daily discharges have varied significantly along the years during this period, between 57 m^3 s^{-1} (in September) and 1740 m^3 s^{-1} (in January). However, a single extraordinary flood event in December 1998 caused the maximum averaged daily discharge to reach 5726 m^3 s^{-1}.

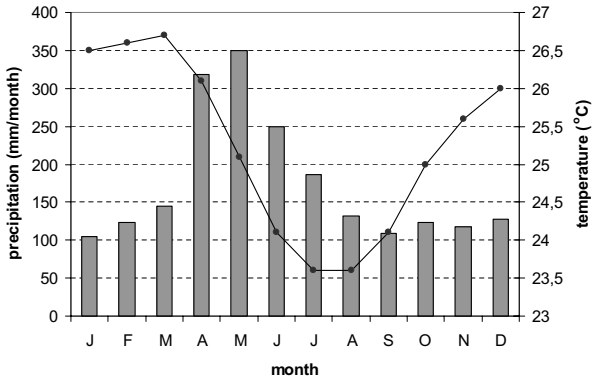

Figure 4 – Monthly mean precipitation and air temperature based on 30 years averages for Salvador (1961-1990).

The other two main catchments, Rio Jaguaripe (2200 km^2) and Rio Subaé (600 km^2) (Fig. 1) are coastal, and have their discharge maxima around June, with mean monthly discharges of 28 m^3 s^{-1} and 9 m^3 s^{-1}, respectively. These values are about three times larger than their discharge minima values of 13 m^3 s^{-1} and 3 m^3 s^{-1} in the summer. The other 91 peripheral catchments (total area of 1713 km^2) have their average flow rate assessed as 34 m^3 s^{-1} (CRA, 2000). The annual variation of the monthly averaged discharge of the peripheral catchments was assessed via the variation of the average monthly precipitation relative to the annual mean. A discharge maximum of 67 m^3 s^{-1} should occur in May, and a minimum of 19 m^3 s^{-1} should occur in January.

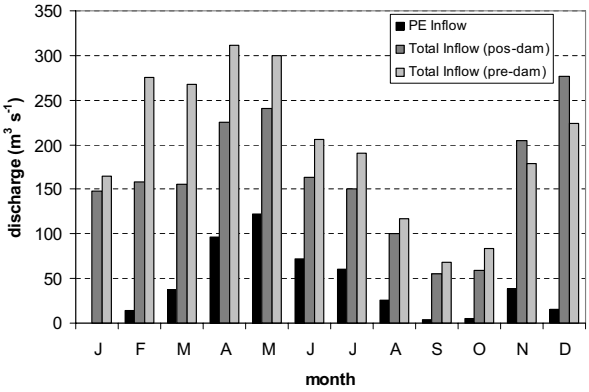

Figure 5 – Monthly mean distribution of the freshwater inflow into BTS. The freshwater inflow is the sum of precipitation-evaporation (PE) and fluvial discharges and is presented for two distinct periods, prior (light gray) and after (dark gray) the construction of Pedra do Cavalo dam. The PE alone, for comparison purposes, is presented in black.

The overall freshwater balance for the BTS, including both atmospheric-water and fluvial discharges, is presented in Figure 5. It is observed that the higher freshwater inflow rates (more than 250 m^3 s^{-1}) occurred between February and May prior to the damming of Rio Paraguaçu. For the pre-dam period, the minimum inflow rates occurred in September, with 68 m^3 s^{-1}, while the year average discharge was 199 m^3 s^{-1}. With the completion of Rio Paraguaçu dam, summer discharges were reduced and the higher monthly averages (more than 200 m^3 s^{-1}) now occur in April and May as well as in November and December. The minimum month-average inflow in September has been reduced to 55 m^3 s^{-1} while the year average discharge shrank 19%, reaching a value of 162 m^3 s^{-1}. The actual maximum monthly average freshwater discharge into the bay (277 m^3 s^{-1}) accounts for less than 0.4% of the equinoctial spring tidal prism.

METHODOLOGY

The data set used in this paper is mainly derived from the **Projeto Bahia Azul**. The data was collected in two different periods, during the summer (dry) season, between January 12 and 28, 1999 and during the winter (wet) season, between May 22 and June 6, 1999. For both periods, data was obtained by: (i) moored oceanographic stations distributed over the BTS and associated coastal region sampling water temperature, salinity, pressure and velocity fields continuously in 17 stations; (ii) meteorological stations measuring wind speed and direction in 4 locations in and outside the bay; (iii) hydrographic surveys sampling water properties over one complete tidal cycle (13 hours), during spring and neap tides, in 12 stations distributed in and outside the bay. Figure 2 shows the location of all the instruments (station 21 was included in the winter campaign). The moored oceanographic stations had either one or two instruments in the moored line. In the former, the instrument was located at mid-water depth while in the latter the instruments were positioned near the surface and close to the bottom (generally 15% and 85% of the water total depth, respectively). The configuration described here does not apply for stations 8 and 9, where ADCP's were moored.

The velocity field was measured with three different types of current meters: (i) 16 *Aanderaa RCM-7* and one *RCM-8*; (ii) 10 *InterOcean S4* and (iii) 2 300 kHz *RDI WorkHorse ADCP's*. The ADCP's were deployed at the bottom and set up to resolve depth-cells of 2 m, scanning at 2 Hz and recording a 3 minutes average current every 15 minutes. The same set up was used with the *InterOcean S4's*, but the RCM's recorded the average current every 5 minutes.

The pressure field, converted to elevation, was sampled with 3 high-resolution *SeaBird SBE* 26 and 5 high-resolution (0.4 cm) pressure sensors installed in some of the *InterOcean S4* (see Fig. 2). S4 data was obtained at 2 Hz and averaged values were recorded at 15 minutes intervals. A similar configuration was applied to the SBE's, except that the data was read at a frequency of 4 Hz. It is anticipated that such set up reduced tidal ranges by cutting both high and low water levels.

In order to extend the tidal elevation coverage inside the bay, three other sets of tide gauge data (Cachoeira, Najé and Aratu in Fig. 2) were obtained from the Oceanographic Data Base coordinated by DHN. Data from Najé and Cachoeira were recorded simultaneously for 15 days in July 1976, whereas a 30 days long data set from Baía de Aratu was collected in May 1988. Mechanical tide gauges were used in all three stations, allowing for 1 hour

reading intervals. In addition, a one-year long time series of tidal elevation (also derived from one-hour reading intervals of tidal charts), obtained from Salvador Harbor in 1960 was included in the data set in order to provide a better characterization of the magnitude of sub-tidal sea level oscillations inside the bay.

Harmonic analyses were performed for both sea level and velocity records in order to quantity the influence of tidal circulation. The methodology adopted was based on Franco (1988).

The hydrographic surveys were performed with 4 SBE19 Sea Cat CTD's, lowered into the water 3 minutes prior to the beginning of measurements. The recording frequency was 2 Hz.

In order to characterize possible seasonal variations in the atmospheric circulation pattern, wind data was sampled at every 15 minutes in 3 different locations (4 for the winter) during the 2 seasonal sampling periods. The positions of these weather stations, named Itaparica, Ilha dos Frades, Mar Grande and Amaralina (wintertime only) are shown in Figure 2. The wind speed (U) was converted to wind stress (τ) using the formulation $\tau = \rho_\alpha C_D |U| U$ (Trenberth et al., 1989), where $\rho_\alpha = 1.2$ kg m^{-3} is the air density and C_D is the drag coefficient, which is a function of U.

OCEANOGRAPHIC CHARACTERISTICS

The wind field

Table 1 presents the mean and the standard deviation wind stress for summer and winter. During summer, the prevailing easterlies generated mean stress values between -0.022 Pa and -0.039 Pa, with standard deviation values comparable to the mean. During the winter, southerly winds were more frequent due to the arrival of cold fronts. The mean values for the prevailing north-south component during winter varied from 0.014 Pa to 0.029 Pa with standard deviations higher than the mean. The Servain climatology (Servain et al., 1996) for the Tropical Atlantic was also used to verify whether the observed values were representative of a normal seasonal pattern or not. It is observed that although there is a good agreement in terms of direction, the estimates for the prevailing component turned out to be 10% to 20% smaller. However, the observed values were comparable to the climatological fields presented by Castro & Miranda (1998), based on the Samuels and Cox GFDL Global Oceanographic Data Set Atlas.

Tides

Tides in the BTS are characteristically semi-diurnal (Tables 2 and 3), with Form number varying between 0.06 in the most internal part of the bay to 0.11 in the adjacent oceanic region. The astronomical tides explained at least 97.5% (station 15) of the variance in the elevation signal, and more conspicuously in the winter.

Tidal ranges increase up bay by a factor of 1.5. M_2 amplitude grows from 0.67 m in the ocean (stations 13 and 14) to 0.89 m in the center of the bay (station 5), 0.93 m in the bay's northern cove and Canal de Itaparica (stations 20 and 17) and 1.06 m at Baía de Iguape (station 18) as indicated in Figure 6a. Inside Rio Paraguaçu, M_2 amplitude is reduced to 1.00 m in Najé and to 0.99 m in Cachoeira, the most inland gauging station. Maximum spring tide ranges in January 1999 underwent an amplification of 1.1 m inside the bay (Fig. 7), from 1.86 m in the ocean (station 13) to 2.94 m in Baía de Iguape (station 18), the location of the largest tide range.

M_2 phase angles among the stations were inconsistent due to different lengths of the time series, different time of data sampling and differences in time and elevation resolution between mechanical tide gauges and electronic pressure sensors. For instance, M_2 phase angle derived from a year-long time series in Salvador differs in 9° from that calculated at station 19 (during summer and winter periods), located in the opposite side of Canal de Salvador. Considering the stations presented in Tables 2 and 3 as reference, the integration of M_2 phase angle within the bay (Figure 6b) shows that the phase grows from 102° in the ocean to 106° in the center of the bay (station 5) to 110° at the mouth of Rio Subaé. Towards Rio Paraguaçu, phase angle reaches 114° at Baía de Iguape and a maximum of 134° at Cachoeira. Along Canal de Itaparica, the phase grows up to 114° at station 17 showing that a tidal convergence point exists in the proximities of station 17.

Along with amplification, the tidal wave undergoes gradual distortion with rising tides increasingly longer (Fig. 7). This pattern of tidal asymmetry occurs everywhere inside the BTS but along Rio Paraguaçu. The average asymmetry (given as the ratio between the rising time and the falling time) grows from 1.03 at station 19 (Canal de Salvador) to 1.23 at station 18 (Baía de Iguape), where the falling tide can be as short as 5 hours. As a result, the high-tide time lag (in relation to the ocean) grows from 30 minutes at station 5 to 45 minutes at station 20 and up to 1.25 hours at station 18. Time lags at low tide are therefore smaller, being 30 minutes at stations 5 and 20 and 45 minutes at station 18.

Tidal asymmetry up Rio Paraguaçu changes its pattern from a longer rising to a longer ebbing tide. Lessa et al. (2000) ascribed this phenomena to friction effect caused by the shallow fluvial delta that progrades into Baía de Iguape. Very low tide levels during spring tides significantly reduce the overall channel depth

Table 1 – Values of wind stress (mean ± standard deviation) estimated from wind speed data obtained from the weather stations located within the BTS during the seasonal sampling periods (see Figure 1 for the location of the weather stations). The monthly mean values from the Servain Climatology (related to the closest location available at 13°S and 39°W and over the years of 1964 to 1988) are also presented for comparison purposes. Unit is Pa.

Site	Summer			
	Date	Wind stress (Pa)		Prevailing direction
		E-W	N-S	
Ilha dos Frades	06/01/99 – 26/01/99	–0.039 ± 0.035	0.016 ± 0.031	ESE
Itaparica	06/01/99 – 16/01/99	–0.038 ± 0.029	0.011 ± 0.016	ESE
Mar Grande	06/01/99 – 10/01/99	–0.022 ± 0.018	0.003 ± 0.015	E
Servain Climatology	January	–0.046	–0.013	ENE
	Winter			
Amaralina	24/05/99 – 10/06/99	0.003 ± 0.017	0.029 ± 0.030	S
Ilha dos Frades	22/05/99 – 02/06/99	0.004 ± 0.009	0.014 ± 0.024	SSW
Itaparica	23/05/99 – 01/06/99	0.009 ± 0.016	0.014 ± 0.018	SSW
Mar Grande	24/05/99 – 10/06/99	–0.002 ± 0.009	0.025 ± 0.026	S
Servain Climatology	June	–0.054	0.035	ESE

Table 2 – Summary of tidal harmonics (for the 7 most important constituents) during the summer sampling period. Amplitude is H (cm), phase lag of equilibrium tide at Greenwich is G (°) and tidal Form number (F) is given by the ratio $F = (K_1 + O_1)/(M_2 + S_2)$.

Site	Q_1	O_1	K_1	N_2	M_2	S_2	M_4	Form Number
	H/G	H/G	H/G	H/G	H/G	H/G	H/G	
S5	2.9/099	6.4/137	3.7/236	9.9/089	89.3/101	31.3/121	2.0/358	0.08
S11	1.6/148	6.1/112	3.9/208	10.0/107	68.6/087	24.1/097	–	0.11
S13	2.1/090	6.7/116	3.5/205	10.5/089	67.0/090	24.9/103	1.2/136	0.11
S14	2.2/101	6.3/119	3.2/198	11.1/089	67.0/090	24.2/104	0.0/136	0.10
S15	3.4/090	7.5/138	3.8/210	10.1/098	92.7/100	31.7/118	7.1/343	0.09
S18	3.0/112	6.7/137	4.0/224	11.4/100	106.0/109	37.9/129	9.6/285	0.07
S19	2.4/100	6.9/126	3.5/210	10.1/097	81.2/101	29.1/118	2.0/234	0.09
S20	2.7/102	7.3/131	4.1/219	10.6/098	93.3/104	33.5/123	3.7/279	0.09

Table 3 – Same as Table 2, but for the winter sampling period.

Site	Q_1	O_1	K_1	N_2	M_2	S_2	M_4	Form Number
	H/G	H/G	H/G	H/G	H/G	H/G	H/G	
W12	1.1/121	5.6/125	3.5/200	9.6/098	66.9/103	28.1/114	0.8/143	0.10
W13	1.4/095	5.9/115	3.6/197	9.6/095	66.5/102	27.4/116	1.2/162	0.10
W14	0.1/058	4.7/124	3.6/195	10.0/094	66.4/102	27.0/115	1.3/170	0.09
W15	0.5/086	4.2/122	3.5/197	13.0/101	90.3/109	38.3/123	4.3/007	0.06
W17	0.7/089	5.3/118	4.1/200	14.3.103	93.0/118	39.4/134	5.7/290	0.07
W18	0.8/072	5.6/116	3.5/197	15.5/095	104.4/110	45.4/128	8.6/293	0.06
W19	1.0/094	5.6/116	3.7/197	11.5/092	79.7/102	33.9/117	1.8/242	0.08
W20	1.1/094	5.5/114	3.4/200	13.3/092	91.2/106	39.5/122	3.5/287	0.07

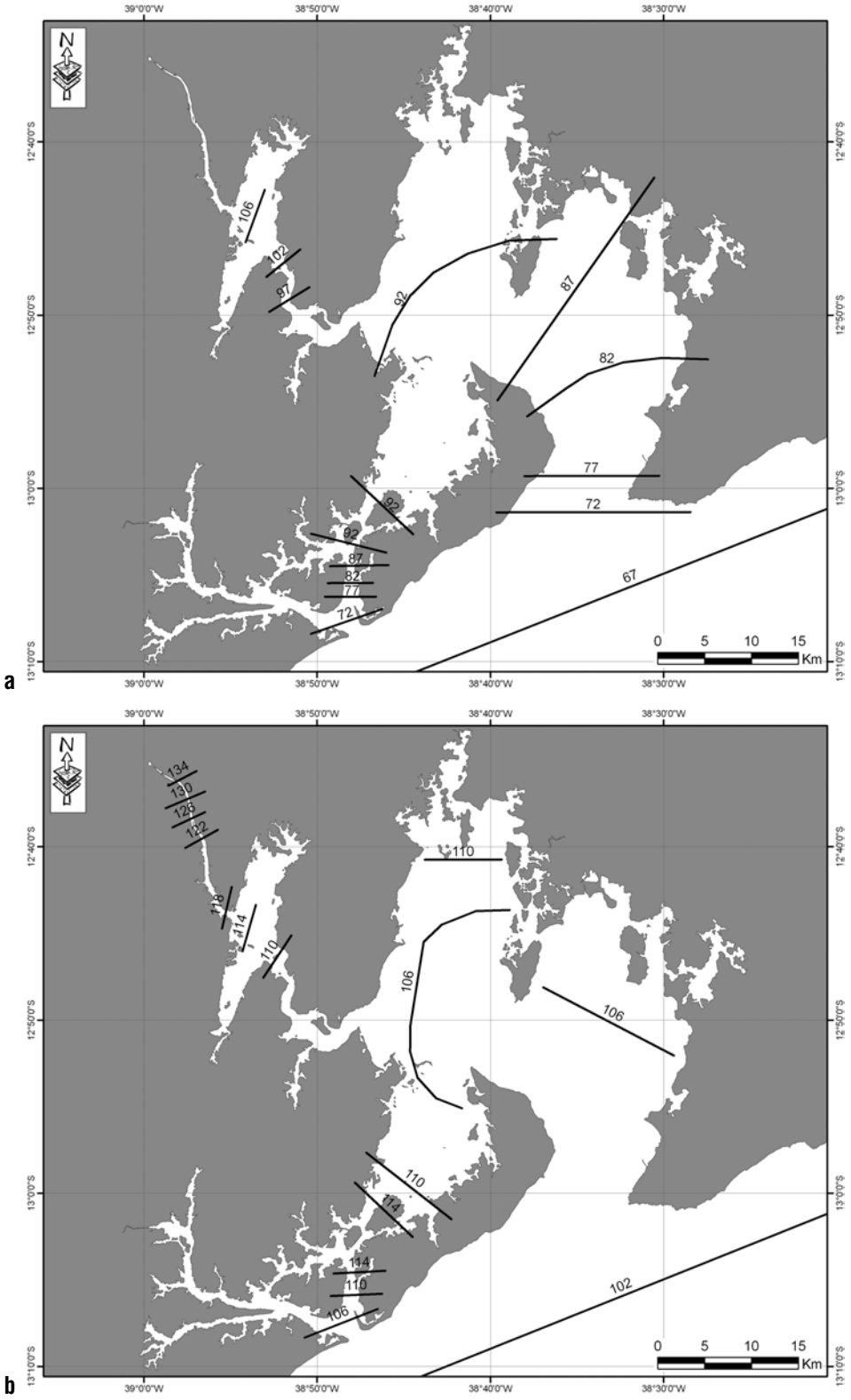

Figure 6 – Cotidal lines of a) amplitude (top panel) and b) phase (bottom panel) showing a progressive amplification and delay of M_2 component into the bay. Units are cm for amplitude and degrees for phase.

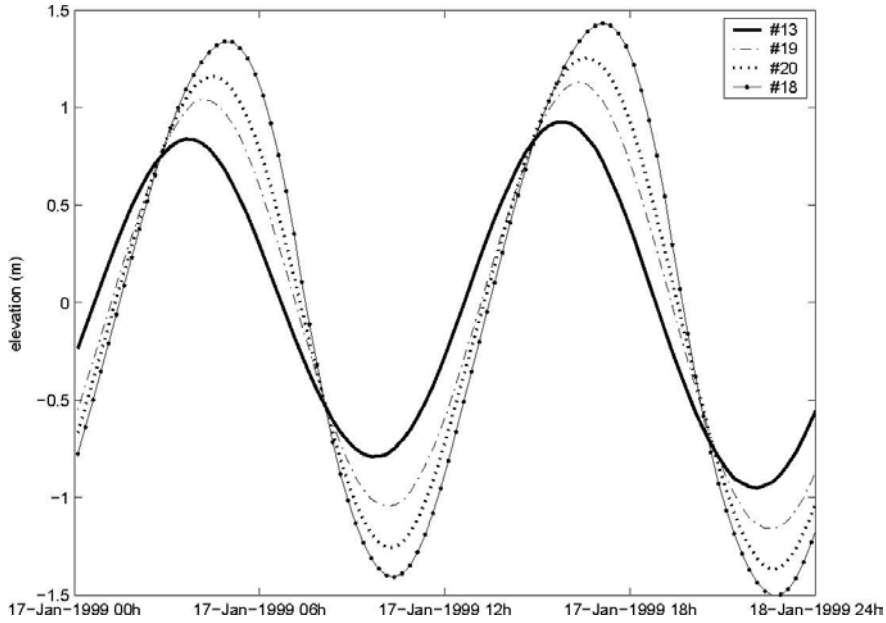

Figure 7 – Simultaneous tidal records in 5 stations located between the ocean and Baía de Iguape (station 18), showing the tidal wave amplification and distortion inside the BTS. See Figure 2 for the station locations.

across the delta enhancing friction and retarding the ebb flow. As a result, rising spring tides can be as short as 5 hours and time lags between Cachoeira and Baía de Iguape are 1 hour at high tide and 3 hours at low tide. Tables 2 and 3 show the growth of M_4 as a result of increasing the tidal asymmetry.

The analysis of the year-long time series from Salvador shows maximum tidal ranges of 2.7 m during an equinoctial-spring tide. The use of a low-pass filter with a cut-off of 72 h revealed about 27 long-period waves up to 20 cm in height with an average period of 12 days. This period is coincident to a 13 days-cycle highlighted by the spectrum analysis of the tide series. These waves were superimposed to a longer period oscillation of 9-10 months with amplitude of 7 cm. The highest and lowest mean sea levels were found to occur during May and October, respectively.

Sub-inertial oscillations during the summer and winter sampling periods had heights of 10 and 17 cm respectively (Fig. 8a,b). The degree of coupling between the shelf and bay oscillations was higher during the winter (with more frequent southerly winds) when at least two waves up to 18 cm in height and a period of 5-6 days could be observed both along the shelf and inside the bay. In the summer (easterlies prevailing winds) the mean sea level trend in the shelf (two oscillations) is matched by the trend observed in the eastern half of the bay (station 19). It becomes, however, quite different from the pattern observed in the most inland stations (18 and 20) where an almost continuously rising trend existed. At Baía de Iguape (station 18) the oscillation (4 cm in height) between January 23 and 26 was apparently caused by a river flood that began on the 23rd and reached a discharge peak of 1512 $m^3\ s^{-1}$ on January 25, 1999.

Tidal currents

The currents inside the BTS (stations 1-8 and 15-21) are clearly tide driven. The correlation coefficient and the variance explanation between the predicted and observed currents, for the component closer to the orientation of the main axis, are above 0.90 and 86%, respectively (Table 4). These numbers decrease as a function of the increasing distance from the bay mouth, reaching values as low as of 0.23 and 4.9% at station 14 during winter. Figure 9 and Figure 10 show the current time series at stations 17 (inside Canal de Itaparica), 13 and 14 (both outside BTS) for summer and winter, respectively. The tidal signal at station 17 is obscured at station 13 (in line with Canal de Salvador) and becomes indiscernible at station 14, mainly in the winter.

Harmonic analysis of the current field inside the BTS (Tables 5 and 6) shows vector Form numbers smaller than 0.19, which characterize the tidal currents as semi-diurnal (Pond & Pickard, 1983). For some stations outside the BTS, such as station 13, the tidal currents are mixed with semi-diurnal predominance, resulting in inequalities between the currents during the highs and lows

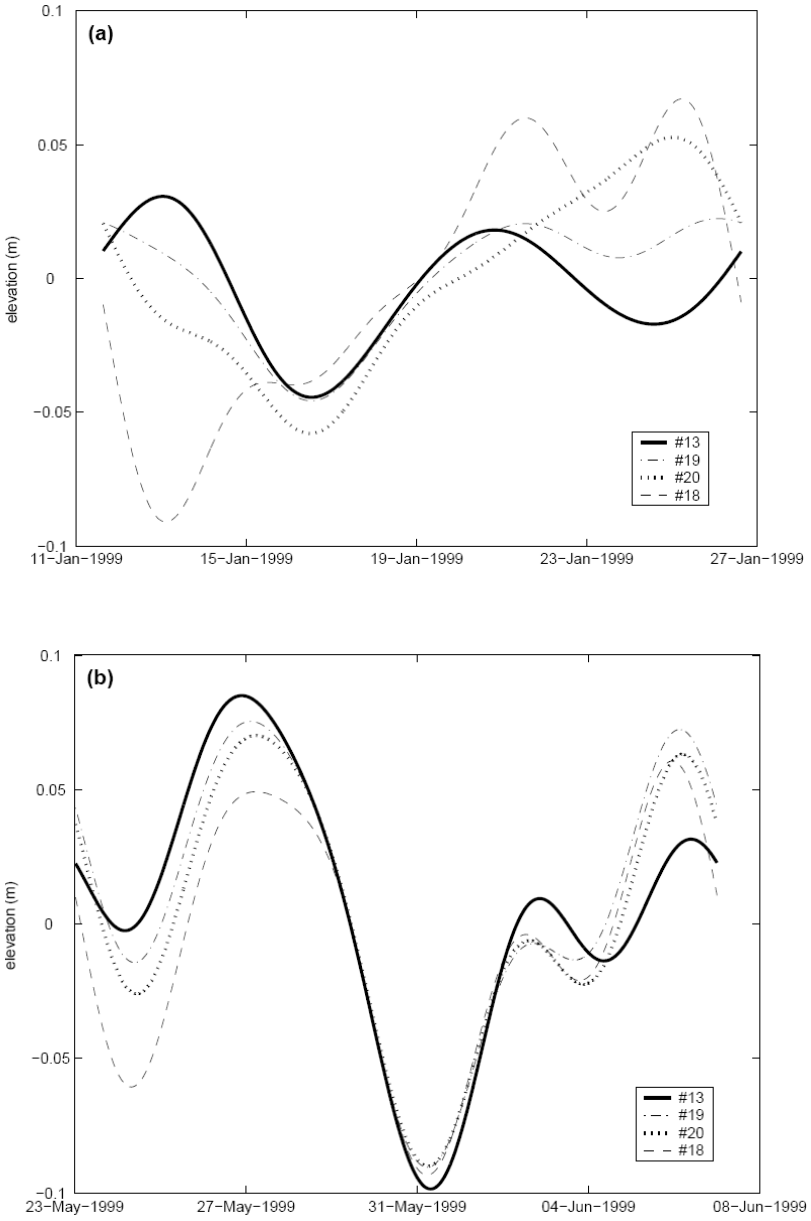

Figure 8 – Time series of the sub-inertial elevation variation for some stations in and outside the bay during a) summer and b) winter.

for each day. At station 14, the tidal currents are still mixed, but here they have diurnal predominance, with vector Form numbers close to 2.4 (the magnitude of the O_1 and K_1 tidal ellipses are very small and of order of few cm s^{-1} only). M_2 and S_2 tidal ellipses in both seasons are shown in Figure 11. In general, the ellipses are oriented along the main channels of the bay and eccentricity tends to be small. For the locations where the water column was sampled in two depths, the orientation of the ellipses did not vary more than a few degrees. Apart from station 15 (located at Canal de Madre de Deus in Figure 2), vertical shear was not significant.

Maximum current velocities occur at the two entrances of the bay, Canal de Salvador (station 8) and Canal de Itaparica (station 17), where the M_2 component close to the surface had magnitudes of 65 cm s^{-1} and 51 cm s^{-1}, respectively. The S_2 component had values of 28 cm s^{-1} and 24 cm s^{-1} for these same locations. Other regions of relatively intense flow were the center of the bay (station 5), with magnitudes of 35 cm s^{-1} for M_2 and 17 cm s^{-1} for S_2, and the channel at station 15, where M_2 and S_2 magni-

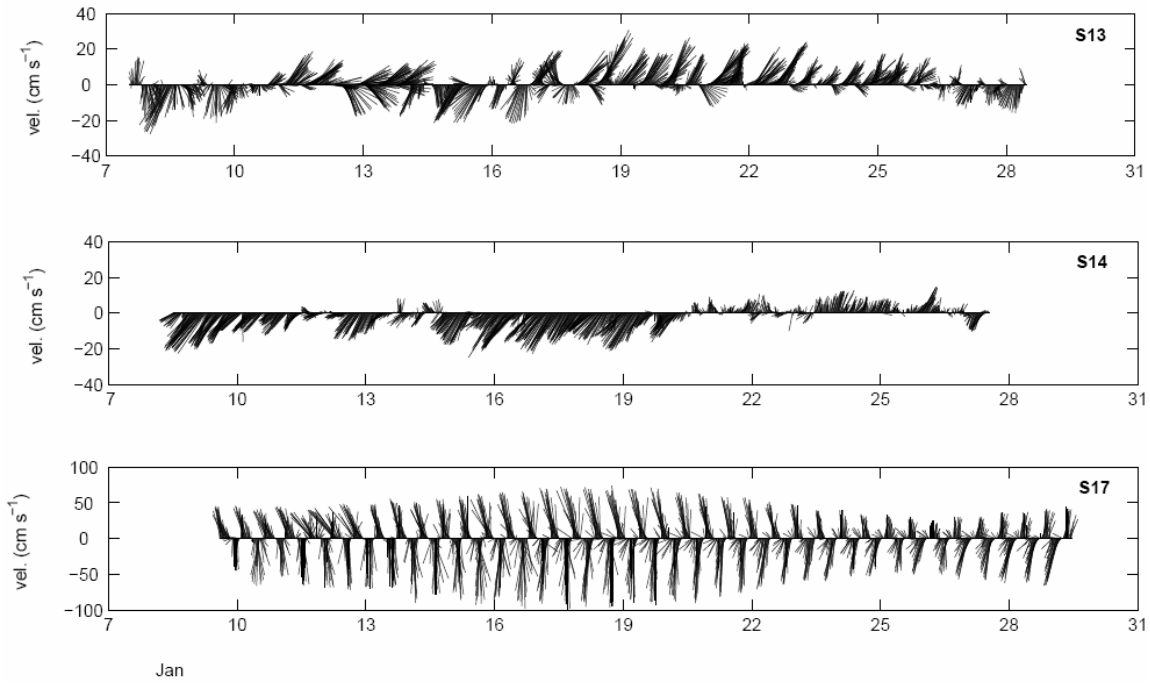

Figure 9 – Time series of the current vectors at stations 13 (top), 14 (middle) and 17 (bottom) during the summer and according to the location map presented in Figure 2. The vectors are related to the true north.

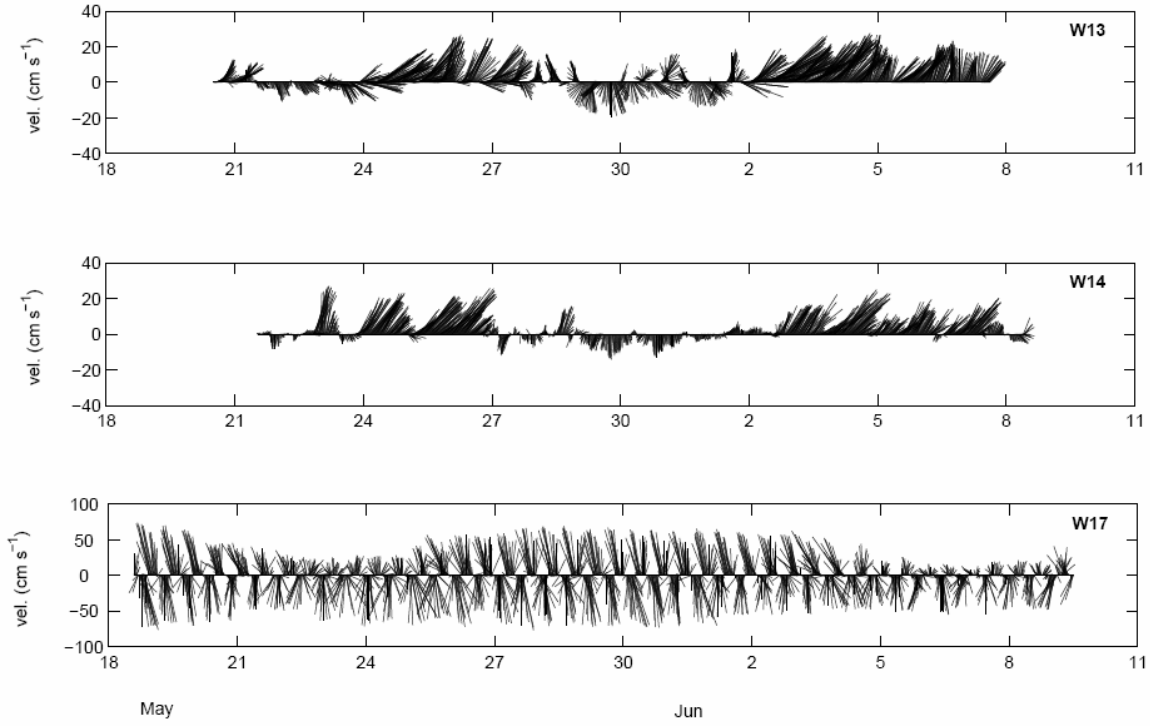

Figure 10 – Same as Figure 9, but for the winter.

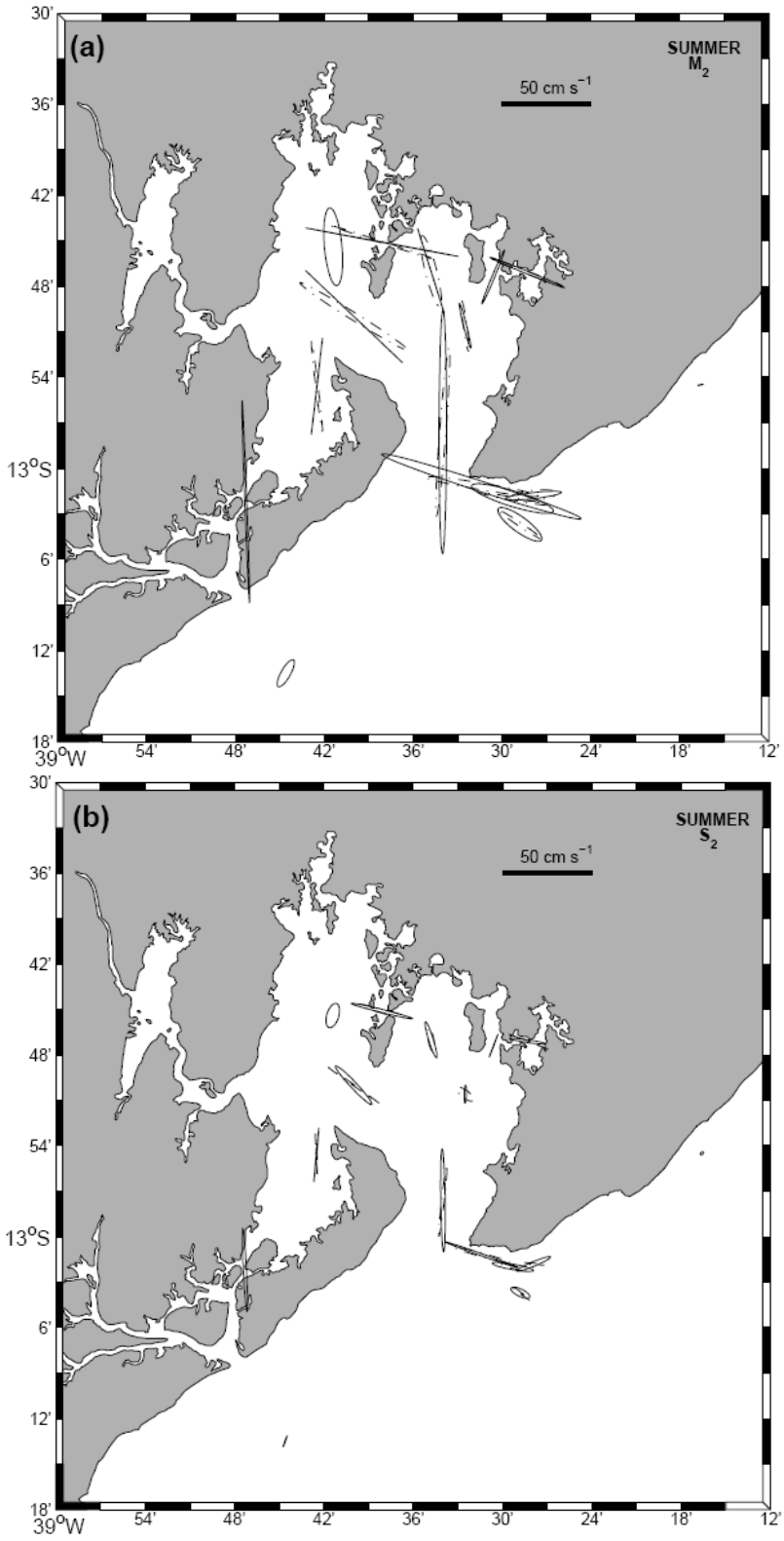

Figure 11 – Harmonic current ellipses for (a) M_2 and (b) S_2 components during summer. All the ellipses are drawn to the same scale.

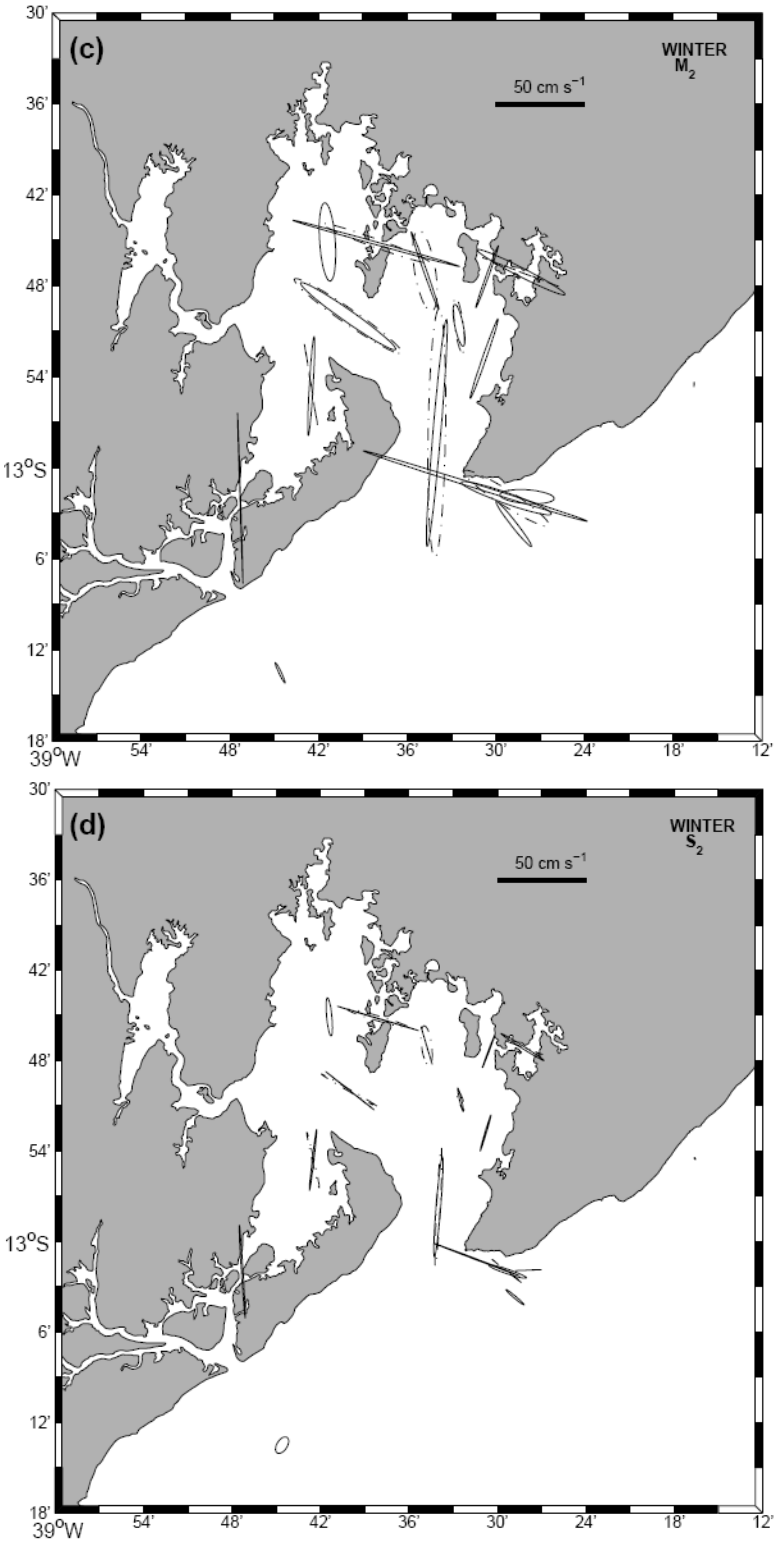

Figure 11 (continued) – Figures (c) and (d) are the same as in (a) and (b), but for the winter. Solid lines indicate either a single current meter or the near surface current meter, while dashed lines represent the near bottom instruments. All the ellipses are drawn to the same scale.

Table 4 – Correlation coefficient and percentage of variance explanation between the predicted time series (based on the harmonic analysis) and the observed currents. The analysis are made in terms of U (east-west oriented) and V (north-south) components of velocity. The orientation angle for the major axis (M axis) is related to true north and rotates clockwise. Single instrument moorings had the current meter located at mid-depth, while the others had surface (S) and bottom (B) instruments located at 15% and 85% of the water depth.

Site		Summer					Winter				
		U comp.		V comp.		M axis	U comp.		V comp.		M axis
		Var %	c. coef.	Var %	c. coef.		Var %	c. coef.	Var %	c. coef.	
01		65.6	0.78	96.9	0.98	177	44.1	0.64	98.2	0.98	176
02	S	90.7	0.94	99.1	0.99	162	79.1	0.87	95.6	0.97	161
	B	87.6	0.93	96.9	0.99	164	73.2	0.85	96.1	0.97	172
03	S	99.0	0.98	84.4	0.91	108	95.9	0.98	89.9	0.95	118
	B	95.6	0.97	81.4	0.89	110	91.8	0.97	79.8	0.90	110
05	S	98.9	0.99	99.7	0.99	135	96.0	0.98	91.9	0.96	126
	B	98.8	0.98	96.9	0.98	122	95.3	0.98	92.4	0.96	123
06	S	42.9	0.65	94.2	0.96	170	38.3	0.59	86.4	0.90	170
	B	60.7	0.76	93.6	0.97	165	23.9	0.48	90.6	0.93	175
07	S	59.2	0.76	97.9	0.98	6	44.8	0.65	96.0	0.97	5
	B	44.8	0.66	98.8	0.98	174	55.8	0.75	92.4	0.97	168
08	S	30.5	0.46	99.9	0.99	0	58.6	0.77	97.3	0.99	5
	B	55.1	0.70	99.2	0.99	4	27.6	0.52	97.9	0.99	2
09	S	85.4	0.92	73.0	0.85	103	82.4	0.91	66.6	0.81	106
	B	88.7	0.94	50.2	0.68	100	38.1	0.62	19.8	0.45	115
10	S	98.3	0.99	97.7	0.98	108	96.0	0.98	92.4	0.96	108
	B	97.2	0.98	87.8	0.92	100	–	–	–	–	–
11	S	66.4	0.81	30.5	0.52	69	54.0	0.72	19.4	0.39	80
	B	79.0	0.89	24.3	0.46	85	–	–	–	–	–
12	S	44.6	0.66	43.9	0.66	73	36.1	0.58	52.1	0.71	86
	B	84.2	0.92	73.2	0.85	124	–	–	–	–	–
13		24.7	0.50	52.1	0.69	44	9.9	0.29	25.1	0.48	50
14		12.1	0.34	8.7	0.29	42	3.7	0.17	4.9	0.23	37
15	S	98.4	0.99	80.2	0.88	101	97.0	0.99	86.5	0.92	106
	B	95.6	0.98	84.7	0.92	107	95.1	0.97	89.5	0.92	108
16		80.8	0.91	92.2	0.96	23	77.5	0.87	90.8	0.94	21
17		46.8	0.59	97.8	0.99	178	29.9	0.51	96.4	0.98	177
21		–	–	–	–	–	81.6	0.88	96.4	0.97	18

tudes near surface were 46 cm s^{-1} and 21 cm s^{-1}, respectively. Since data was collected in two different periods, the current values presented in the text refer to an average between the summer (Table 5) and winter values (Table 6). Considerable vertical shear occurs at station 15 (local depth of 25 m), with near-surface flow about 40% higher than the flow near the bottom (32 cm s^{-1} for M_2 and 16 cm s^{-1} for S_2). Apart from these locations, the strength of the flow throughout the bay (stations 1 to 3, 6, 7 and 16) was generally moderate with the M_2 and S_2 components ranging from 12 cm s^{-1} to 28 cm s^{-1} and 5 cm s^{-1} to 17 cm s^{-1}, respectively. Outside the BTS, moderate tidal currents were restricted to stations 9 to 12, where M_2 component was higher than 13 cm s^{-1}. At station 10, flow canalization between the coast and the ebb tidal delta gave rise to M_2 component of 62 cm s^{-1} at the surface. During the summer, where data was collected in two different depths, a significant vertical shear was observed, with near bottom current velocities 50% smaller than those observed at the surface. Away from the bay, the tidal influence was only of significance at station 13 (velocity up to 8.5 cm s^{-1} for M_2), apparently due to its alignment with the Canal de Salvador.

Table 5 – Summary of the harmonic analysis (O_1, K_1, M_2, S_2 components) for the velocity field during the summer sampling period. M and m are the amplitude (cm s^{-1}) of the major and minor axes, respectively, G is the Greenwich phase and θ is the direction of the major axis (relative to true north and clockwise). The last column is the associated vector Form number given by the ratio $F = (K_1 + O_1)/(M_2 + S_2)$.

Site		O_1		K_1		M_2		S_2		Form Number
		M/m	°G/°θ	M/m	°G/°θ	M/m	°G/°θ	M/m	°G/°θ	
S1		2.0/0.3	074/358	1.8/0.3	284/133	21.5/4.9	031/355	6.9/3.4	254/198	0.13
S2	S	1.8/0.8	236/126	2.1/1.0	275/133	24.4/0.0	029/342	10.4/1.3	031/342	0.11
	B	2.4/1.3	217/132	2.4/0.6	292/127	20.2/3.2	018/345	6.7/1.6	026/348	0.18
S3	S	1.1/0.5	066/097	0.6/0.1	197/103	22.6/0.7	208/292	10.1/0.8	224/278	0.05
	B	1.6/1.2	246/306	0.7/0.1	055/290	20.9/0.8	181/291	12.0/0.2	232/291	0.07
S5	S	3.4/0.4	070/351	2.2/0.8	113/354	37.2/0.0	045/313	14.7/1.8	064/316	0.11
	B	2.3/0.5	197/109	3.2/0.1	312/115	35.5/2.1	023/301	17.3/0.3	046/305	0.10
S6	S	1.8/0.8	225/213	0.4/0.2	036/265	12.7/0.9	021/345	5.0/0.6	217/182	0.12
	B	1.7/0.5	310/064	2.1/1.1	006/057	14.2/1.0	011/352	5.6/2.1	205/127	0.19
S7	S	1.8/0.0	090/200	0.9/0.3	321/008	26.5/0.1	039/187	14.8/0.1	236/005	0.06
	B	1.5/0.1	035/156	1.2/0.1	219/199	24.9/0.7	038/173	11.6/0.2	062/177	0.07
S8	S	4.0/0.7	225/204	2.2/0.5	326/181	67.0/2.1	033/000	28.3/1.3	047/359	0.06
	B	3.0/0.4	061/321	1.4/0.2	168/315	46.4/1.8	208/184	20.0/0.8	049/006	0.07
S9	S	3.3/0.3	340/246	1.8/0.2	001/260	24.1/4.3	215/107	11.7/1.5	206/100	0.14
	B	1.4/0.9	210/093	1.0/0.5	038/081	19.5/0.8	197/100	7.5/0.8	201/106	0.09
S10	S	1.7/0.1	323/280	0.6/0.0	255/145	58.8/2.8	186/108	21.6/0.6	008/289	0.03
	B	2.5/0.4	342/282	0.8/0.1	279/106	32.5/1.8	357/279	16.0/1.0	010/285	0.07
S11	S	2.8/0.8	140/033	2.5/0.7	302/257	15.9/1.7	219/084	10.2/1.2	226/068	0.20
	B	2.3/1.1	171/123	0.8/0.4	198/281	13.4/2.9	209/084	6.1/0.4	209/095	0.16
S12	S	1.7/0.7	049/229	1.8/0.3	038/295	14.9/4.2	194/125	5.8/2.0	213/115	0.17
	B	2.0/0.5	025/337	1.8/0.3	188/306	14.8/1.0	206/123	6.9/0.4	207/127	0.17
S13		3.6/0.2	322/094	2.1/0.3	007/096	8.5/2.6	006/030	3.2/0.1	211/200	0.49
S14		3.6/0.4	217/046	2.7/0.0	257/043	1.5/0.1	031/258	1.1/0.7	251/221	2.44
S15	S	0.6/0.2	360/160	0.9/0.2	250/152	43.6/0.1	027/280	17.7/0.9	206/104	0.03
	B	0.5/0.1	025/012	0.4/0.2	143/278	31.5/0.5	205/108	13.7/1.2	203/105	0.02
S16		0.8/0.2	352/035	0.6/0.1	253/182	16.1/0.8	206/203	6.7/0.1	207/201	0.06
S17		0.8/0.2	258/032	1.0/0.1	190/177	55.5/0.6	303/358	22.9/0.9	297/357	0.02

The tidal wave behaved as a standing wave throughout the bay. A departure from a standing wave propagation was observed at station 7, at the entrance of Canal de Itaparica, where two velocity peaks occurred during the rising tides (except at neaps). The second, and strongest, velocity peak was ascribed to the inundation of relatively high intertidal areas along Canal de Itaparica. As observed by Lessa (2000) in macrotidal estuaries, the inundation of large intertidal areas late in the rising tide causes a sharp increase of the tidal prism and flow acceleration.

In accordance with the pattern of tidal elevation asymmetry, predicted tidal currents were clearly ebb orientated in most of the stations, exceptions being stations 2, 16, 15 and 21, where stronger currents were flood orientated. The ratio between maximum ebb to maximum flood currents at stations 17, 7, 5, and 8 varied between 1.09 (station 5 in the winter, v_{ebb} = 50 cm s^{-1}) and 1.43 (station 17 in the summer, v_{ebb} = 110 cm s^{-1}). At the bay mouth (station 8), maximum ebb-currents (114 cm s^{-1}) were up to 1.33 times higher than maximum flood currents.

Table 6 – Same as Table 5, but for the winter sampling period.

Site		O_1		K_1		M_2		S_2		Form Number
		M/m	°G/°θ	M/m	°G/°θ	M/m	°G/°θ	M/m	°G/°θ	
W1		1.0/0.2	124/050	1.2/0.5	113/061	21.6/4.4	032/356	10.6/1.5	045/354	0.07
W2	S	1.5/0.1	059/018	1.1/0.7	015/174	22.6/0.9	035/340	10.8/0.0	045/343	0.08
	B	1.3/0.2	238/210	1.0/0.4	120/076	22.5/5.9	028/350	11.1/2.9	031/352	0.07
W3	S	1.4/0.2	356/114	0.5/0.0	276/312	27.7/2.5	218/296	14.3/0.7	212/302	0.05
	B	0.6/0.1	032/093	1.2/0.4	229/278	23.0/0.1	009/110	12.2/0.1	036/110	0.05
W5	S	1.8/0.7	204/162	1.5/0.3	173/279	32.5/3.3	225/124	17.2/0.1	240/128	0.07
	B	1.2/0.2	250/307	0.4/0.3	035/064	36.5/4.1	017/304	18.6/0.6	038/300	0.03
W6	S	1.6/0.3	218/146	0.7/0.0	303/167	11.7/2.4	037/348	6.7/0.5	033/346	0.13
	B	1.4/0.1	009/245	1.6/0.0	328/240	15.3/2.4	176/172	5.9/1.3	012/339	0.14
W7	S	1.6/0.1	202/010	1.5/0.2	279/360	27.2/1.1	226/003	17.0/0.5	238/007	0.07
	B	1.1/0.3	179/350	1.3/0.0	270/006	23.5/0.1	037/171	15.7/0.6	239/347	0.06
W8	S	2.0/0.6	256/193	2.0/0.0	302/225	62.6/2.2	032/005	27.7/1.3	046/005	0.04
	B	4.1/0.6	020/008	1.8/0.5	038/046	68.4/4.9	038/001	32.9/1.0	051/003	0.06
W9	S	2.5/0.4	333/284	1.8/0.4	185/251	26.8/3.0	205/109	11.1/1.2	213/108	0.11
	B	4.6/1.9	009/246	8.2/1.6	308/091	28.3/4.3	205/122	11.1/0.2	034/307	0.32
W10	S	5.5/0.3	327/286	2.2/0.3	137/287	66.0/1.1	187/107	25.7/0.2	193/110	0.08
W11	S	3.5/0.9	169/088	2.4/0.1	002/087	15.3/3.8	215/094	7.3/0.0	214/088	0.26
W12	S	2.8/1.1	360/286	0.8/0.4	145/234	15.9/1.6	022/321	6.6/0.6	206/129	0.16
W13		1.5/0.7	080/017	1.7/0.4	121/108	6.2/0.7	208/154	5.1/2.9	356/033	0.28
W14		3.0/0.1	230/189	1.2/0.2	047/208	1.2/0.1	276/182	0.6/0.2	036/332	2.37
W15	S	1.4/0.3	150/128	1.2/0.1	091/286	48.6/0.8	211/105	23.9/0.1	031/286	0.04
	B	1.1/0.4	287/260	0.5/0.2	128/300	32.3/2.3	209/109	17.9/1.4	220/106	0.03
W16		0.4/0.1	159/107	0.9/0.3	173/026	18.2/0.7	209/200	9.5/0.3	219/201	0.05
W17		0.9/0.2	212/350	1.2/0.1	343/360	46.7/0.2	132/178	25.6/0.5	128/176	0.03
W21		1.0/0.8	357/330	1.2/0.3	107/052	23.2/1.1	206/200	10.4/0.4	224/197	0.07

Residual circulation

The residual circulation inside the bay over a 15 day period is presented in Figure 12 and shows a similar pattern for both summer and winter periods. As a result of the dominance of the tidal forcing, the velocities did not exceed 5 cm s^{-1} (a parcel moving with this speed would advect substances as far as 65 km over this period). At the northern part of BTS, significant flow occurred only at Canal de Madre de Deus (station 15), where both current meters registered northwest currents of order of 5 cm s^{-1} and at Baía de Aratu (station 3), where the residual flow was towards the bay at both depths. Residual velocities found at stations 16 and 2, inside the channels leading to Baía de Aratu and Ilha de Madre de Deus, also registered northward bound residual flows.

The residual circulation at station 5 is characterized by near-surface currents opposing the direction of the near-bottom currents, both in the summer and winter. The flow was directed down-bay close to the surface and up-bay near the bottom, with velocities of order of 5 cm s^{-1}. This suggests a permanent pattern in this area that is likely related to gravitational circulation. A slightly similar pattern was observed at station 8 in the summer, with near-surface and near-bed currents offset by about 120°.

South bound residual currents were recorded by all current meters at stations 7 and 17, inside the Canal de Itaparica, with velocities up to 6 cm s^{-1} at station 17. These residual vectors suggest that a possible anti-clockwise residual flow could exist around Ilha de Itaparica.

In the inner shelf, the residual circulation is clearly seasonal and the winds may be ascribed to as an important mechanism for driving the currents. Exceptions are the channel areas between the mainland and the ebb-tide delta at station 10 where strong residual currents flowed towards the bay in both seasons (15 cm s^{-1} in summer and 10 cm s^{-1} in winter), and station 13, where the

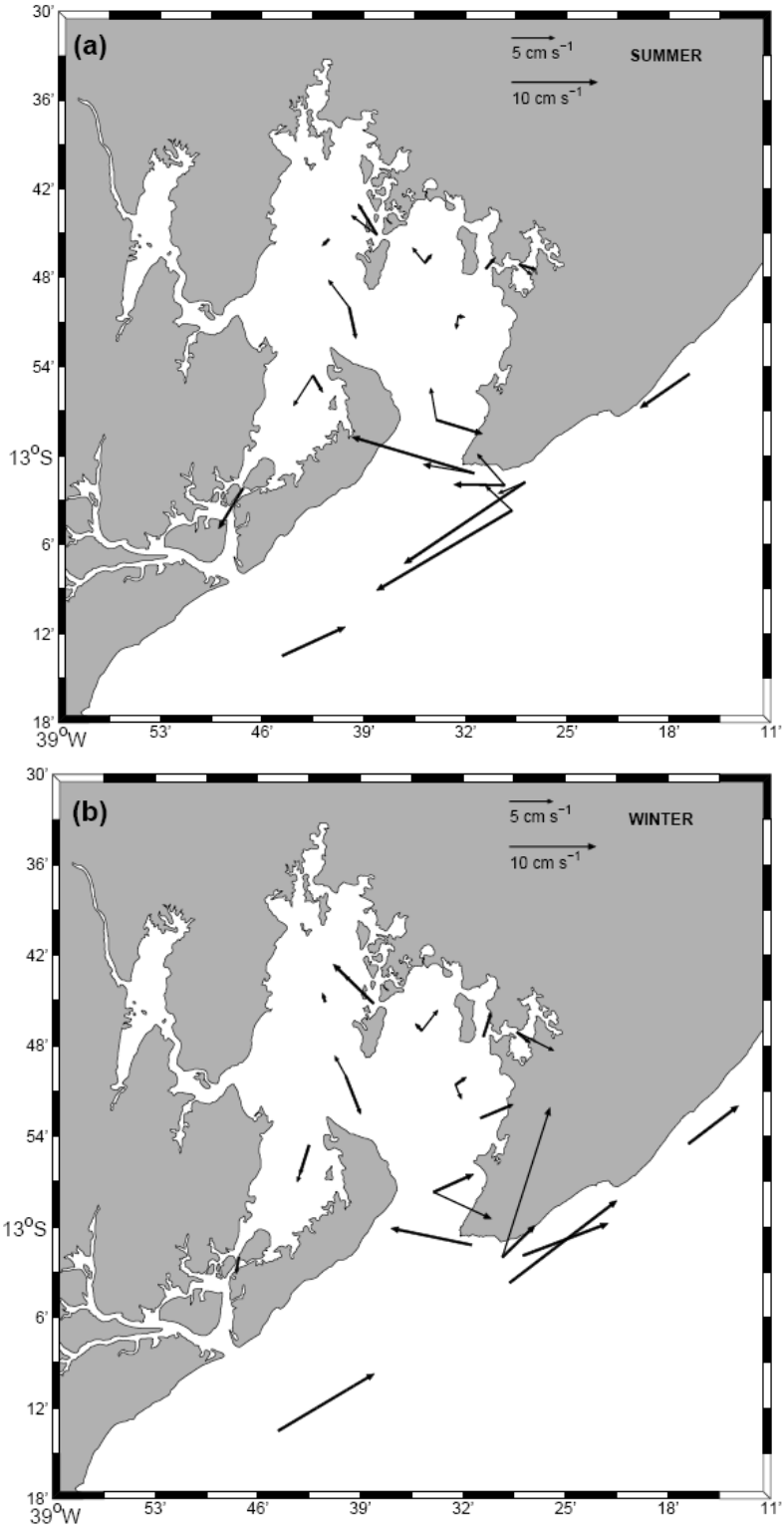

Figure 12 – Residual velocities during (a) summer and (b) winter. Tick line vectors represent either a single current meter or the near surface current meter, whereas the narrow line vectors represent the near bottom instrument. Vector scales of 5 cm s^{-1} and 10 cm s^{-1} are drawn at the upper right part of the panels.

flow was persistently directed to the northeast. In this later case, however, the velocity varied significantly between seasons, being more intense during winter.

For the other locations, a change in the predominant wind direction, from easterlies during summer to southerlies during winter (Table 1), forced a change in the residual current direction. These changes are ascribed to the more frequent arrival of cold fronts in winter (e.g., Chaves, 1999; Amorim, 2005). Near-bottom currents in the summer period were weaker than those near the surface at stations 10 to 12, indicating a significant velocity shear in the water column (those near-surface currents were above 15 cm s^{-1} and more than three times larger than the near-bottom currents). The onshore flow close to the bottom at these locations and the strong near surface flow towards southwest may be an indication of an upwelling favorable system during this season. At station 14, the mid-depth current also agreed with this summertime southwestward circulation showing a magnitude of 7 cm s^{-1}. The lack of near-bottom current estimates at stations 11 and 12 during winter prevented any comparison with the summertime observations.

Water properties

In the summer (Tables 7 and 8), the largest difference in the mean surface temperature (3°C) occurred during the spring tide, between the warmest surface waters of the most inland point (station 1, T = 29.9°C) and the relatively colder surface waters at the ocean stations (stations 9 to 12, 26.9° $<$ T $<$ 27.3°C). Along the water column, mean temperature differences were less than 1°C for most stations inside the bay, but reached 1.7°C outside the bay at station 12 (Table 7). Temperature standard deviations for all stations were also of order of few decimals of a degree.

Mean salinity in the shelf was always above 37, with negligible vertical gradients. The bay was dominated by oceanic water with mean salinities higher than 36.4 and very little vertical variation. The only exception was station 4 (in front of the Canal do Rio Paraguaçu), which presented a surface mean salinity of 35.6. Very high salinities were found at station 3, inside Baía de Aratu (see Figure 2), where relatively high evaporation rate may occur, as suggested by the mean temperatures being higher than the surrounding stations.

In the winter period (Tables 9 and 10), the temperature was quite homogeneous in the water column and differentiated little among the stations in and outside the bay. The maximum difference in the mean surface temperature was 0.7°C (Table 9) and the largest vertical difference was 0.3°C at station 12. On the other hand, the horizontal variation of the surface mean salinity varied up to 4.2 (Table 10) between the inland most station and the ocean. This is clearly related to the higher winter precipitation rates along the coast. Vertical salinity gradients were also more pronounced, with differences of more than 1 between surface and bottom in various stations inside the bay.

Figure 13 shows the vertical and horizontal salinity and temperature variations (mean $\pm$ one standard deviation) along a line through the center of the bay connecting stations 4, 5 and 8. It shows gradual changes along this line and different spatial trends between these fields. Whereas the temperature increased up-bay both in the summer and the winter, salinity decreased. Moreover, larger horizontal and vertical variations occurred during summer for temperature and during winter for salinity. If one standard deviation is considered, maximum temperature and salinity variations between any point in water column at stations 8 and 4 can be 2°C (summer) and 3°C (winter), respectively. Seasonally, maximum salinity variation in the water column was about 2.2 at station 8, 3.2 at station 5 and 3.9 at station 4. For these respective stations, maximum seasonal temperature variation was close to 2.4°C, 3.2°C and 3.6°C.

SUMMARY AND DISCUSSION

Based on the available data analyzed, the hydrodynamics of the study region was clearly separated in two different systems, the BTS itself and the connected inner shelf. Different seasonal scenarios regarding water properties and circulation patterns were also observed. Inside the BTS, the circulation was mostly tide driven throughout the year, but water properties did change noticeably between summer and winter.

During the summer (dry season), the water inside the bay was considerably warmer than the oceanic waters in the adjacent continental shelf, and horizontal temperature variations between the two regions could be as large as 3°C. The surface temperature could be as high as 30°C at the northernmost part of the BTS. Horizontal salinity variations in the dry season were not pronounced and surface waters below 36 were only found at the mouth of Rio Paraguaçu (mean of 35.6). A still largely sediment-infilled bay, along with small precipitation rates within a semi-arid catchment area corresponding to 95% of the total, allows for high water salinities to be observed in the eastern half of the bay. The waters on the inner shelf had surface salinity above 37. According to Emilson (1961), the water mass in the BTS (and along the associated shelf) during the summer could be classified as Tropical Water – TW (temperatures above 20°C and salinities above 36).

Table 7 – Mean temperature and salinity and ± 1 standard deviation for the stations where water properties were collected during a complete tidal cycle (neap situation) for the summer sampling period. The water depths are surface and bottom (local depth is between parenthesis).

Site	Temperature (°C)			Salinity		
	Surface	Bottom		Surface	Bottom	
S1	29.9 ± 0.22	29.6 ± 0.09	(6 m)	36.6 ± 0.04	36.6 ± 0.03	(6 m)
S2	29.7 ± 0.29	29.1 ± 0.16	(13 m)	36.8 ± 0.04	36.9 ± 0.06	(13 m)
S3	30.0 ± 0.36	29.6 ± 0.04	(26 m)	37.1 ± 0.03	37.2 ± 0.05	(26 m)
S4	29.8 ± 0.28	29.4 ± 0.03	(16 m)	35.6 ± 0.22	36.2 ± 0.04	(16 m)
S5	29.4 ± 0.27	28.6 ± 0.10	(26 m)	36.6 ± 0.08	36.8 ± 0.01	(26 m)
S6	29.2 ± 0.23	28.5 ± 0.03	(22 m)	36.9 ± 0.01	36.8 ± 0.02	(22 m)
S7	29.2 ± 0.26	28.8 ± 0.09	(31 m)	36.7 ± 0.01	36.7 ± 0.01	(31 m)
S8	28.4 ± 0.32	28.1 ± 0.07	(38 m)	37.0 ± 0.07	37.0 ± 0.03	(38 m)
S9	27.7 ± 0.14	27.2 ± 0.25	(28 m)	37.0 ± 0.04	37.2 ± 0.01	(28 m)
S10	27.8 ± 0.20	27.3 ± 0.21	(18 m)	37.1 ± 0.03	37.2 ± 0.02	(18 m)
S11	28.0 ± 0.35	27.0 ± 0.19	(28 m)	37.2 ± 0.06	37.2 ± 0.03	(28 m)
S12	27.9 ± 0.27	26.2 ± 0.14	(34 m)	37.2 ± 0.01	37.2 ± 0.01	(34 m)

Table 8 – As in Table 7, but during a spring tidal cycle.

Site	Temperature (°C)			Salinity		
	Surface	Bottom		Surface	Bottom	
S1	29.9 ± 0.44	29.6 ± 0.21	(6 m)	36.4 ± 0.03	36.4 ± 0.03	(6 m)
S2	29.4 ± 0.24	28.8 ± 0.07	(14 m)	36.8 ± 0.09	36.8 ± 0.08	(14 m)
S3	29.3 ± 0.23	29.1 ± 0.09	(30 m)	37.0 ± 0.01	37.0 ± 0.03	(30 m)
S4	29.7 ± 0.26	29.2 ± 0.24	(18 m)	35.6 ± 0.21	36.2 ± 0.16	(18 m)
S5	29.1 ± 0.31	28.5 ± 0.14	(29 m)	36.4 ± 0.13	36.7 ± 0.06	(29 m)
S6	28.9 ± 0.22	28.3 ± 0.07	(23 m)	36.8 ± 0.04	36.8 ± 0.01	(23 m)
S7	28.9 ± 0.26	28.7 ± 0.04	(30 m)	36.6 ± 0.03	36.6 ± 0.03	(30 m)
S8	28.0 ± 0.42	27.7 ± 0.09	(38 m)	36.9 ± 0.09	37.0 ± 0.06	(38 m)
S9	26.9 ± 0.26	26.2 ± 0.33	(25 m)	37.1 ± 0.07	37.2 ± 0.03	(25 m)
S10	27.1 ± 0.21	26.5 ± 0.31	(19 m)	37.1 ± 0.05	37.2 ± 0.05	(19 m)
S11	27.0 ± 0.32	25.9 ± 0.06	(29 m)	37.2 ± 0.02	37.3 ± 0.01	(29 m)
S12	27.3 ± 0.26	26.0 ± 0.24	(31 m)	37.2 ± 0.02	37.2 ± 0.02	(31 m)

During winter (wet season), the horizontal temperature variation between the ocean and the bay was reduced to less than 1°C (surface mean temperatures varying from 26.5°C to 27.1°C). On the other hand, the horizontal salinity difference increased, with values as large as 4. For the northernmost part of the BTS, the surface mean salinity could be as low as 32.3, while values above 36 were found at the inner shelf. This less salty and relatively cold waters found inside the BTS gave rise to a so called coastal water mass (CW), that inhibited the penetration of TW into the bay. This CW was observed in the inner shelf (stations 9, 10, 11 and 12) with thickness varying from 5 to 10 m.

The seasonal formation of CW appears to be entirely related to the discharge of the smallest catchments areas around the bay (as well as direct precipitation), since the discharge from Rio Paraguaçu reaches its lowest value between May and July. The average monthly discharges from Rio Paraguaçu in January and May 1999 were 9.9 $m^3 s^{-1}$ and 11.3 $m^3 s^{-1}$, respectively. Extreme discharges from Rio Paraguaçu are, however, likely to affect the salinity structure as far as station 4. Genz et al. (2006) monitored a simulated 8-day flood event with water being released by Pedra do

Table 9 – As in Table 7, but during the winter sampling period.

Site	Temperature (°C)			Salinity		
	Surface	Bottom		Surface	Bottom	
W1	26.8 ± 0.21	26.7 ± 0.08	(7 m)	32.7 ± 0.22	33.0 ± 0.16	(7 m)
W2	26.7 ± 0.18	26.6 ± 0.04	(11 m)	33.7 ± 0.15	34.5 ± 0.26	(11 m)
W3	27.1 ± 0.24	26.9 ± 0.06	(30 m)	33.4 ± 0.22	34.1 ± 0.12	(30 m)
W4	26.7 ± 0.12	26.6 ± 0.04	(13 m)	32.7 ± 0.20	34.2 ± 0.07	(13 m)
W5	26.6 ± 0.14	26.5 ± 0.00	(29 m)	33.7 ± 0.12	34.9 ± 0.03	(29 m)
W6	26.7 ± 0.10	26.6 ± 0.00	(23 m)	34.3 ± 0.02	34.9 ± 0.03	(23 m)
W7	26.6 ± 0.14	26.5 ± 0.01	(26 m)	33.2 ± 0.48	34.6 ± 0.04	(26 m)
W8	26.4 ± 0.14	26.5 ± 0.02	(34 m)	35.0 ± 0.15	35.3 ± 0.07	(34 m)
W9	26.6 ± 0.15	26.5 ± 0.02	(30 m)	35.8 ± 0.08	36.6 ± 0.02	(30 m)
W10	26.5 ± 0.11	26.5 ± 0.01	(19 m)	35.7 ± 0.15	36.2 ± 0.46	(19 m)
W11	26.6 ± 0.17	26.5 ± 0.03	(30 m)	35.7 ± 0.10	36.7 ± 0.04	(30 m)
W12	26.5 ± 0.18	26.6 ± 0.08	(33 m)	35.8 ± 0.13	36.8 ± 0.10	(33 m)

Table 10 – As in Table 8, but during the winter sampling period.

Site	Temperature (°C)			Salinity		
	Surface	Bottom		Surface	Bottom	
W1	27.0 ± 0.35	26.6 ± 0.06	(7 m)	32.3 ± 0.36	33.5 ± 0.30	(7 m)
W2	26.7 ± 0.12	26.6 ± 0.04	(12 m)	33.7 ± 0.28	34.4 ± 0.31	(12 m)
W3	26.9 ± 0.23	26.8 ± 0.06	(30 m)	32.4 ± 0.54	34.2 ± 0.11	(30 m)
W4	27.1 ± 0.32	26.7 ± 0.10	(12 m)	33.1 ± 0.21	33.9 ± 0.23	(12 m)
W5	26.7 ± 0.20	26.6 ± 0.01	(29 m)	33.3 ± 0.52	34.7 ± 0.16	(29 m)
W6	26.6 ± 0.12	26.5 ± 0.02	(24 m)	34.2 ± 0.08	34.8 ± 0.09	(24 m)
W7	26.7 ± 0.12	26.6 ± 0.07	(12 m)	34.2 ± 0.11	34.3 ± 0.07	(12 m)
W8	26.5 ± 0.12	26.5 ± 0.05	(37 m)	35.1 ± 0.34	35.7 ± 0.30	(37 m)
W9	26.8 ± 0.27	26.8 ± 0.07	(40 m)	36.3 ± 0.14	37.0 ± 0.06	(40 m)
W10	26.7 ± 0.13	26.6 ± 0.05	(18 m)	36.1 ± 0.22	36.6 ± 0.08	(18 m)
W11	26.7 ± 0.28	26.8 ± 0.03	(29 m)	36.4 ± 0.14	36.9 ± 0.01	(29 m)
W12	26.7 ± 0.25	27.0 ± 0.04	(39 m)	36.5 ± 0.15	37.1 ± 0.03	(39 m)

Cavalo dam, with a maximum discharge of 1534 m^3 s^{-1} (15 times the pre-dam average discharge). The maximum discharge coincided with high water spring (3.3 m tide range in Baía de Iguape) and caused a surge of 0.5 m close to the river mouth inside the Baía de Iguape. This surge was imperceptible at the gauging station in São Roque (see location in Figure 1). The salinity field, however, was influenced along the whole extent of Canal do Paraguaçu. A well-mixed water column (vertical salinity variation of 0.3), with surface value of 32.4 at the end of the channel, became partially mixed (vertical variations of 5.2), with surface salinity of 27.2. In scenarios like this, the Baía de Iguape and secondarily the Canal do Paraguaçu, act as a buffer region against the Rio Paraguaçu floods. Short-lived river floods are almost completely damped inside the bay. Surface salinity gradients, reaching up to 8 psu km-1 during a flood event, were found inside the Baía de Iguape (Genz et al., 2006).

An estimate of the flushing time for the innermost station where CTD profiles were performed (stations 1 and 4 in Fig. 2) was done analytically based on the conservation of salt and volume (Miranda et al., 2002) and according to the equation

$$T_f = [(S_0 - \bar{S})/S_0](V/Q_f).$$

S_0 and $\bar{S}$ represent salinity at the oceanic and innermost stations, respectively. V is the volume of the bay associated with the flushing process, which is equal to 1.1 $\times$ 10^{10} m^3 and Q_f is the freshwater discharge. Typical values for S_0,

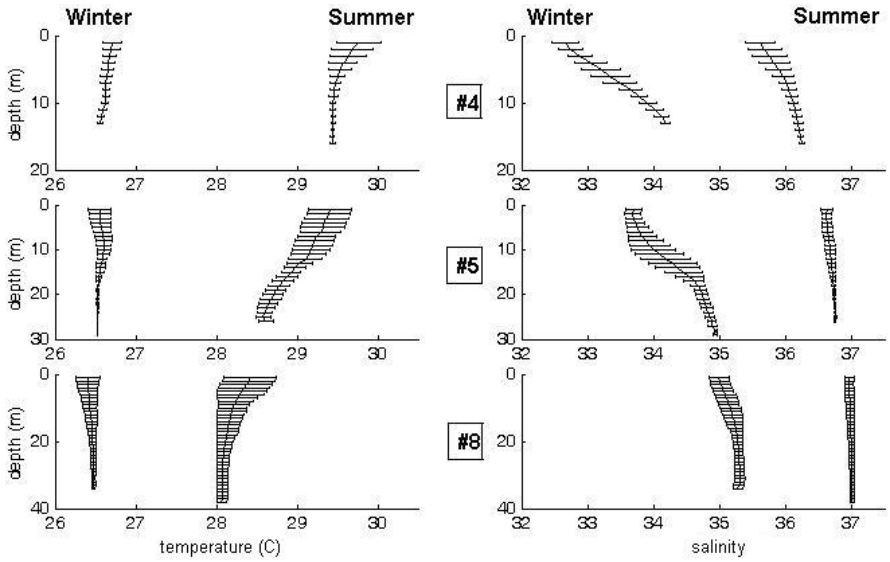

Figure 13 – Schematic representation of vertical profiles for the mean (thick line) temperature and salinity during summer and winter at Rio Paraguaçu mouth (station 4), in the center of the BTS (station 5) and at the entrance of the bay (station 8) for a complete tidal cycle (13 hours). The gray areas represent $\pm$ 1 standard deviation from the mean value.

$\bar{S}$ and Q_f for January (May) 1999 are 37.2 (36.2), 35.6 (32.5) and 89.0 (345.5) $m^3\ s^{-1}$, respectively. These parameters indicate that due to the small freshwater inflow, the flushing time in summer ($\sim$62 days) is about 1.7 times longer than that in winter ($\sim$38 days).

When compared to other relevant coastal bays in Brazil, the BTS is likely to be the one with the longest flushing time, given its high ratio between volume and freshwater discharge (0.32×10^8 s $< V/Q_f <$ 1.2×10^8 s for the central area of the bay). For example, Baía de Guanabara, according to Kjerfve et al. (1997), has a V/Q_f ratio twice as small, varying from 0.12×10^8 s to 0.67×10^8 s in the dry and wet season, respectively. A V/Q_f ratio of 0.12×10^8 s was also estimated for Baía de Paranaguá, considering a year average freshwater input of about 200 $m^3\ s^{-1}$ (Lessa et al., 1998; Mantovanelli et al., 2004). Due to the large flushing times it is recommended that proper management policies regarding the disposal of urban and industrial waste into the BTS must be adopted.

The total freshwater inflow into the BTS was reduced after the construction of Pedra do Cavalo dam (mean annual discharge dropped from 199 $m^3\ s^{-1}$ to 162 $m^3\ s^{-1}$). This reduction, however, is not entirely related to the effects of the dam, since the inflow was also diminished during the winter when Rio Paraguaçu would normally account for less than 30% of the total freshwater input. Longer trends (20-30 year cycles) in precipitation and river discharges, as pointed out by Pekarova et al. (2003) are more likely to be the reason for the observed reduction of the fresh water inflow into the BTS after 1985.

While the circulation did not vary significantly between seasons inside the bay, a clearly seasonal pattern was observed at the associated inner shelf. During the summer, the easterly winds drove sub-inertial currents parallel to the coastline and towards southwest mostly, except for the station in front of Canal de Itaparica. The near bottom onshore flow (stations with two current meters) associated with the presence of relatively cold waters at the bottom (when compared to the values found during the winter) is an indication of an upwelling process. In the winter, the arrival of cold fronts and the associated reversal of the wind direction generated events of northeast currents which, depending on the wind persistence, would dominate the residual circulation. A similar pattern of seasonal circulation was observed by Lessa & Cirano (2006) at the southern coast of Bahia and by Amorim (2005) at about 100 km south of the BTS.

The seasonal variations imposed by the changes in the meteorological forcing also affect the sub-inertial oscillations in the BTS and at its vicinity. During summer the BTS is less affected by the easterlies and the oscillations in the most inland portion of the bay can be decoupled from those observed at the inner shelf. This could also be caused by the distinct wind patterns (in and outside the BTS) that can occur during this season. On the other

hand, during winter the more frequent arrival of cold fronts and the longer fetch created in the presence of southerly winds give rise to a strong coupling between the sub-inertial oscillations for the waters inside the BTS and those at the inner shelf.

Due to the orientation of the residual current vectors inside the bay, one would feel tempted to suggest that an anticlockwise circulation is normally established inside the BTS where water moves northward towards station 15 and returns via Canal de Itaparica. However, the spatial density of the current meters deployed inside the bay is far too small, and it is very likely that the residual vectors indicate segments of eddies of much smaller scale. These eddies are normally generated by the interaction of the flow with complex bathymetry and the coastal contours of a water body. Kjerfve et al. (1992) understand that residual circulation gyres arise due to lateral circulation, which in turn are a manifestation of the variability of the current magnitude and direction over short distances. This lateral variability is explained by the presence of prevailing ebb and flood channels within the same cross-section, as demonstrated by Kjerfve & Proehl (1979). Some current meters inside the bay might have been deployed in predominantly flood or ebb channels, either enhancing the expected tidal current asymmetry (station 8) or reversing it (station 21). Therefore, the degree of ebb or flood dominance among the stations is highly dependable on their location. For instance, strong ebb dominance at station 8 is apparently counterbalanced by flood dominance at the western side of Canal de Salvador, where a small flood-tidal delta in front of Mar Grande (see Figure 2 for location) is clearly mapped in the depth charts. The overall stronger ebb-tidal currents are in agreement with the pattern of asymmetry of the tidal wave. Ebb-directed bed-load net sediment transport is thus expected in most areas of the bay, especially those close to large intertidal areas. This direction of net-sediment transport is corroborated by the presence of extensive ebb-tidal deltas in front of Canal de Salvador (Banco de Santo Antonio) and Canal de Itaparica. Also, an ebb-tidal delta internal to the bay, in front of Canal do Paraguaçu, is also an indication of bed-load flushing.

Given the vast amount of data available, the main goal of this paper was to provide a general characterization of oceanographic aspects of the BTS and adjacent areas and identify how these aspects vary during the dry (summer) and the wet (winter) season. Although the circulation driving forces have been described here, several questions remain and need to be elucidated before a satisfactory understanding of the different spatial and temporal scales involved in the physical oceanography of the bay can be achieved. The authors are aware that in this study the region was reasonably well covered in space, but not in time. The temporal coverage (15 days for each season) is far too short for a good description of the seasonality. The results already obtained in this work will be used to plan a more comprehensive observational programs focusing on the study of mass and volume transports for the most important pathways within the bay, as well as the seasonal variation of the water properties within the BTS and its interaction with the coastal zone. A 3D circulation numerical model is already being implemented to help addressing these questions.

ACKNOWLEDGEMENTS

This work was supported by the projects MARBOBA – CTPETRO/CNPq (grant number 502356/2003-0) and SACODE – CTPETRO/CNPq (grant number 550469/2005-2). Further support was also provided by a Brazilian scientific network called REDE 05/01 – PETRORISCO, funded by CTPETRO/FINEP/CNPq. Guilherme C. Lessa was supported by a CNPq research grant. We are thankful to the Environmental Department of the State Government of Bahia (Centro de Recursos Ambientais) for providing all the data sets related to Projeto Bahia Azul. We also thank the two anonymous referees for their thoughtful comments and the technician Rafael Cabral Carvalho for helping with some figures.

REFERENCES

AMORIM FN. 2005. Caracterização oceanográfica da Baía de Camamu e adjacências e mapeamento das áreas de sensibilidade a derrames de óleo. M.Sc. Thesis, Curso de Pós-Graduação em Geologia da Universidade Federal da Bahia. 163 pp.

ANGULO RJ, LESSA GC & SOUZA MC. 2006. A critical review of mid- to Late-Holocene sea-level fluctuations on the eastern Brazilian coastline. Quaternary Sci. Rev., 25(5-6): 486–506.

ANP. Agência Nacional do Petróleo, Gás Natural e Biocombustíveis. 2007. Available at: <http://www.brazil-rounds.gov.br/geral/mapas/JEQ_CAL.pdf>. Access on: November 10, 2007.

ANTAQ. Agência Nacional de Transportes Aquaviários. 2005. Anuário Estatístico Portuário – 2005. Available at: <http://www.antaq.gov.br/NovositeAntaq/estatisticasanuario.asp>. Access on: November 9, 2007.

BITTENCOURT ACDP, DOMINGUEZ JML & USSAMI N. 1999. Flexure as a tectonic control on the large scale geomorphic characteristics of the eastern Brazil coastal zone. J. Coast. Res., 15(2): 505–519.

CASTRO BM & MIRANDA LB. 1998. Physical oceanography of the western Atlantic continental shelf located between 4°N and 34°S. In: ROBINSON AR & BRINK KH (Ed.). The Sea, John Wiley & Sons, Inc., New York, 11: 209–251.

CEPLAB. 1979. Bacias Hidrográficas do Estado da Bahia. Centro de Planejamento da Bahia, Séries Recursos Naturais, Salvador, Bahia, 215 pp.

CHAVES RR. 1999. Variabilidade da precipitação na região Sul do Nordeste e sua associação com padrões atmosféricos. M.Sc. Thesis, Instituto Nacional de Pesquisas Espaciais. 159 pp.

CRA. Centro de Recursos Ambientais. 2000. Saneamento ambiental da Baía de Todos os Santos. Modelamento e avaliação ambiental. Desenvolvimento de modelos computacionais de circulação hidrodinâmica, de transporte de contaminantes e de qualidade de água da BTS, e elaboração do seu diagnóstico. Relatório dos estudos básicos. Technical Report RT-257-03-GR-002-RF, 248 pp., Centro de Recursos Ambientais, Salvador, Bahia, Brazil.

CRA. Centro de Recursos Ambientais. 2001. Saneamento ambiental da Baía de Todos os Santos. Modelamento e avaliação ambiental. Desenvolvimento de modelos computacionais de circulação hidrodinâmica, de transporte de contaminantes e de qualidade da água da BTS. Prognóstico dos efeitos do Programa Bahia Azul com relação à balneabilidade das praias. Technical Report RT-257-05-MA-003-RF, 262 pp., Centro de Recursos Ambientais, Salvador, Bahia, Brazil.

CUPERTINO JA & BUENO GV. 2005. Arquitetura das seqüências estratigráficas desenvolvidas na fase de lago profundo no Rifte do Recôncavo. Bol. Geoc. Petrobras, 13(2): 245–267.

DIAS K. 2004. Reavaliação da distribuição espacial das facies texturais do leito da Baía de Todos os Santos, Undergraduate Thesis, Curso de Graduação em Geologia da Universidade Federal da Bahia. 50 pp.

EMILSON I. 1961. The shelf and coastal waters off Southern Brazil, Bolm. Inst. Oceanogr., São Paulo, 17: 101–112.

FRANCO AS. 1988. Tides: Fundamentals, Analysis and Prediction, São Paulo, Fundação Centro Tecnológico de Hidráulica, 249 pp.

GENZ F. 2006. Avaliação dos efeitos da Barragem de Pedra do Cavalo sobre a circulação estuarina do Rio Paraguaçu e Baía de Iguape. Tese de Doutoramento, Programa de Pós-Graduação em Geologia, Universidade Federal da Bahia, 266 p.

GENZ F, LESSA GC & CIRANO M. 2006. The Impact of an Extreme Flood upon the Mixing Zone of the Todos os Santos Bay, Northeastern Brazil. J. Coast. Res., 39: 707–712.

IBGE. Instituto Brasileiro de Geografia e Estatística. 2006. Estimativas Populacionais para os municípios brasileiros em 01/07/2006. Available at: < http:// www.ibge.gov.br/ home/ estatistica/ populacao/ estimativa2006/default.shtm >. Access on: November 9, 2007.

INMET. Instituto Nacional de Meteorologia. 1992. Normais Climatológicas – 1961 a 1990. Ministério da Agricultura, Pecuária e Abastecimento. 155 pp.

KING LC. 1956. Geomorfologia da Região Oriental do Brasil. Rev. Bras. Geogr., 2: 37–72.

KJERFVE B & PROEHL JA. 1979. Velocity variability in a cross-section of a well-mixed estuary, J. Mar. Res., 37(3): 409–418.

KJERFVE B, SEIM HE, BLUMBERG AF & WRIGHT LD. 1992. Modelling of the Residual Circulation in Broken Bay and the lower Hawkesbury River, NSW, Aust. J. Mar. Freshw. Res., 43: 1339–1357.

KJERFVE B, RIBEIRO CHA, DIAS GTM, FILIPPO AM & QUARESMA VS. 1997. Oceanographic characteristics of an impacted coastal bay: Baía de Guanabara, Rio de Janeiro, Brazil. Cont. Shelf Res., 17(13): 1609–1643.

LESSA GC. 2000. Morphodynamic controls on tides and tidal currents in two macrotidal shallow estuaries, NE Australia. J. Coast. Res., 16(4): 976–989.

LESSA GC, MEYERS S & MARONE E. 1998. Holocene Stratigraphy in the Paranaguá Bay estuary, southern Brazil, J. Sediment. Res., 68(6): 1060–1076.

LESSA GC, BITTENCOURT ACSP, BRICHTA A & DOMINGUEZ JML. 2000. A reevaluation of the late quaternary sedimentation in Todos os Santos Bay (BA), Brazil. An. Acad. Bras. Cienc., 72(4): 573–590.

LESSA GC, DOMINGUEZ JML, BITTENCOURT ACSP & BRICHTA A. 2001. The tides and tidal circulation of Todos os Santos Bay, northeast Brazil: a general characterization. An. Acad. Bras. Cienc., 73(2): 245–261.

LESSA GC & CIRANO M. 2006. On the Circulation of a Coastal Channel within the Abrolhos Coral-Reef System -Southern Bahia (17°40'S), Brazil, J. Coast. Res., 39: 450–453.

LIMA GMP & LESSA GC. 2002. The freshwater discharge in Todos os Santos Bay and its significance to the general water circulation. Revista Pesquisas. Porto Alegre (RS), 28: 85–98.

MANTOVANELLI A, MARONE E, DA SILVA ET, LAUTERT LF, KLINGENFUSS MS, PRATA VP, NOERNBERG MA, KNOPPERS BA & ANGULO RJ. 2004. Combined tidal velocity and duration asymmetries as a determinant of water transport and residual flow in Paranaguá Bay estuary. Estuar. Coast. Shelf Sci., 59(4): 523–537.

MARTIN L, BITTENCOURT ACSP, FLEXOR JM, SUGUIO K & DOMINGUEZ JML. 1986. Neotectonic movements on a passive continental margin: Salvador region, Brazil. Neotectonics, 1: 87–103.

MIRANDA LB, CASTRO BM & KJERFVE B. 2002. Princípios de Oceanografia Física de Estuários, Editora da Universidade de São Paulo, São Paulo, 414 pp.

MONTENEGRO AM, FONSECA CA & CAMPOS EJD. 1999. Implementação do modelo oceânico da Universidade de Princeton para o estudo da circulação e dispersão de materiais na Baía de Todos os Santos, PUC, Ci. Biol. e do Meio Amb., 2: 10–18.

PEKAROVA P, MIKLANEK P & PEKAR J. 2003. Spatial and temporal runoff oscillation analysis of the main rivers of the world during the 19th-20th centuries. J. Hydrol., 274(1-4): 62–79.

POND S & PICKARD GL. 1983. Introductory Dynamical Oceanography. 2nd ed. Butterworth-Heinemann. 329 pp.

SERVAIN J, STRICHERZ JN & LEGLER DM. 1996. TOGA pseudo-stress atlas 1985-1994, volume 1: Tropical Atlantic. Centre ORSTOM, Plouzané, France, 158 pp.

SRH. Superintendência de Recursos Hídricos. 1996. Plano Diretor de Recursos Hídricos – Bacia do Médio e Baixo Paraguaçu, Salvador, Bahia. 195 pp.

THORNTHWAITE CW. 1948. An approach toward a rational classification of climate. Geogr. Rev., 38(1): 55–94.

TRENBERTH KE, OLSON JC & LARGE WG. 1989. A Global Ocean Wind Stress Climatology Based on ECMWF Analyses. Technical Report NCAR/TN-338+STR, National Center for Atmospheric Research, Boulder, Colorado, 98 pp.

TRICART J & DA SILVA TC. 1968. Estudos de Geomorfologia da Bahia e Sergipe, Fund. Desenv. da Ciência na Bahia, Salvador, 167 pp.

WOLGEMUTH KM, BURNETT WC & MOURA PL. 1981. Oceanography and suspended material in Todos os Santos Bay, Rev. Bras. Geoc., 11: 172–178.

NOTES ABOUT THE AUTHORS

Mauro Cirano is an oceanographer (FURG/1991) with a Msc in Physical Oceanography from Instituto Oceanográfico da Universidade de São Paulo (IOUSP/1995) and a PhD in the same area from the University of New South Wales (UNSW), Sydney, Australia (2000). He has been working as an Associate Professor since 2004 at the Universidade Federal da Bahia (UFBA). His research interest is the oceanic circulation, based on data analysis and numerical modeling, area where he has conducting many research projects for the last 15 years, focused on the meso and large-scale aspects.

Guilherme Camargo Lessa has a Geography degree from the Universidade Federal de Minas Gerais (1985) and a Masters in Geography from the Universidade Federal do Rio de Janeiro (1990). He obtained his PhD in Marine Sciences at the University of Sydney (Australia) in 1994. He has worked as a Post-Doc at the Universidade Federal do Paraná and Universidade Federal da Bahia, which he joined as an Associate Professor in 1997. His research interests cover marine sedimentology, coastal and estuarine circulation and coastal (barrier-estuarine) geological evolution.